LETTER

doi:10.1038/nature12730

N^6-methyladenosine-dependent regulation of messenger RNA stability

Xiao Wang[1], Zhike Lu[1], Adrian Gomez[1], Gary C. Hon[2], Yanan Yue[1], Dali Han[1], Ye Fu[1], Marc Parisien[3], Qing Dai[1], Guifang Jia[1,4], Bing Ren[2], Tao Pan[3] & Chuan He[1]

N^6-methyladenosine (m^6A) is the most prevalent internal (non-cap) modification present in the messenger RNA of all higher eukaryotes[1,2]. Although essential to cell viability and development[3–5], the exact role of m^6A modification remains to be determined. The recent discovery of two m^6A demethylases in mammalian cells highlighted the importance of m^6A in basic biological functions and disease[6–8]. Here we show that m^6A is selectively recognized by the human YTH domain family 2 (YTHDF2) 'reader' protein to regulate mRNA degradation. We identified over 3,000 cellular RNA targets of YTHDF2, most of which are mRNAs, but which also include non-coding RNAs, with a conserved core motif of G(m^6A)C. We further establish the role of YTHDF2 in RNA metabolism, showing that binding of YTHDF2 results in the localization of bound mRNA from the translatable pool to mRNA decay sites, such as processing bodies[9]. The carboxy-terminal domain of YTHDF2 selectively binds to m^6A-containing mRNA, whereas the amino-terminal domain is responsible for the localization of the YTHDF2–mRNA complex to cellular RNA decay sites. Our results indicate that the dynamic m^6A modification is recognized by selectively binding proteins to affect the translation status and lifetime of mRNA.

Messenger RNA is central to the flow of genetic information. Regulatory elements (for example, AU-rich element, iron-responsive element), in the form of short sequence or structural motif imprinted in mRNA, are known to control the time and location of translation and degradation processes[10]. Reversible and dynamic methylation of mRNA could add another layer of more sophisticated regulation to the primary sequence[2,11]. m^6A, a prevalent internal modification in the messenger RNA of all eukaryotes, is post-transcriptionally installed by m^6A methyltransferase (for example, MT-A70, Fig. 1a) within the consensus sequence of G(m^6A)C (70%) or A(m^6A)C (30%)[12]. The loss of MT-A70 leads to apoptosis in human HeLa cells[13], and significantly impairs development in *Arabidopsis*[4] and in *Drosophila*[5]. Our recent discoveries of m^6A demethylases FTO (fat mass and obesity-associated protein)[7] and ALKBH5[8] demonstrate that this RNA methylation is reversible and may dynamically control mRNA metabolism. The recently revealed m^6A transcriptomes (methylome) in human cells and mouse tissues showed m^6A enrichments within long exons and around stop codons[14,15], further suggesting fundamental regulatory roles of m^6A. However, despite these progresses the exact function of m^6A remains to be elucidated.

Whereas methyltransferase may serve as the 'writer' and demethylases (FTO and ALKBH5) act as the 'eraser' of m^6A on mRNA, potential m^6A-selective-binding proteins could represent the 'reader' of the m^6A modification and exert regulatory functions through selective recognition of methylated RNA. Here, we show that the YTH-domain family member 2 (YTHDF2), initially found in pull-down experiments using m^6A-containing RNA probes[14], selectively binds m^6A-methylated mRNA and controls RNA decay in a methylation-dependent manner.

The YTH domain family is widespread in eukaryotes and known to bind single-stranded RNA with the conserved YTH domain (>60% identity) located at the C terminus[16,17]. In addition to previously reported YTHDF2 and YTHDF3[14], we also discovered YTHDF1 as another m^6A-selective binding protein by using methylated RNA bait containing the known consensus sites of G(m^6A)C and A(m^6A)C versus unmethylated control (Extended Data Fig. 1a). Further, highly purified poly(A)-tailed RNAs were incubated with recombinant glutathione-*S*-transferase (GST)-tagged YTHDF1-3 and then separated by GST-affinity column. By using a previously reported liquid chromatography-tandem mass spectrometry (LC-MS/MS) method[7,8], we found that the m^6A-containing RNAs were greatly enriched in the YTHDF-bound portion and diminished in the flow-through portion (Fig. 1b and Extended Data Fig. 1b). Gel-shift assay revealed that YTHDF2 has a 16-fold higher binding affinity to methylated probe compared to the unmethylated one, as well as a slight preference to the consensus sequence (Extended Data Fig. 1c, d). This protein was selected for subsequent characterization because it has a high selectivity to m^6A, and was thought to be associated with human longevity[18].

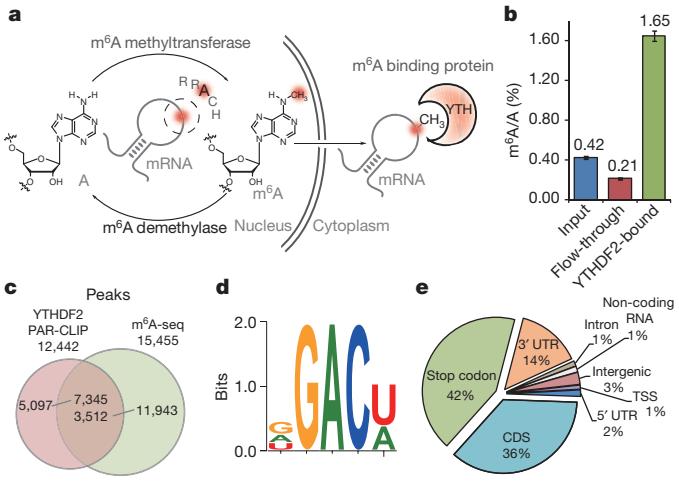

Figure 1 | YTHDF2 selectively binds m^6A-containing RNA. a, Illustration of m^6A methyltransferase, demethylase and binding proteins. RRACH is the extended m^6A consensus motif, where R is G or A and H is not G. **b**, LC-MS/MS showing m^6A enrichment in GST–YTHDF2-bound mRNA while depleted in the flow-through portion. Error bars, mean ± s.d., $n = 2$, technical replicates. **c**, Overlap of peaks identified through YTHDF2-based PAR-CLIP and the m^6A-seq peaks in the same cell line. **d**, Binding motif identified by MEME with PAR-CLIP peaks ($P = 3.0 \times 10^{-46}$, 381 sites were found under this motif out of top 1,000 scored peaks). **e**, Pie chart depicting the region distribution of YTHDF2-binding sites identified by PAR-CLIP, TSS (200-bp window from the transcription starting site), stop codon (400-bp window centred on stop codon).

[1]Department of Chemistry and Institute for Biophysical Dynamics, The University of Chicago, 929 East 57th Street, Chicago, Illinois 60637, USA. [2]Ludwig Institute for Cancer Research, Department of Cellular and Molecular Medicine, UCSD Moores Cancer Center and Institute of Genome Medicine, University of California, San Diego School of Medicine, 9500 Gilman Drive, La Jolla, California 92093-0653, USA. [3]Department of Biochemistry and Molecular Biology and Institute for Biophysical Dynamics, The University of Chicago, 929 East 57th Street, Chicago, Illinois 60637, USA. [4]Department of Chemical Biology and Synthetic and Functional Biomolecules Center, College of Chemistry and Molecular Engineering, Peking University, Beijing 100871, China.

We next applied two independent methods to identify RNAs that are the binding partners of YTHDF2: (1) photoactivatable ribounucleoside crosslinking and immunoprecipitation (PAR-CLIP)[19] to locate the binding sites of YTHDF2; (2) sequencing profiling of the RNA of immunopurified ribonucleoprotein complex (RNP) (RIP-seq)[20] to extract cellular YTHDF2–RNA complexes. Approximately 10,000 crosslinked clusters covering 3,251 genes were identified in PAR-CLIP (Extended Data Fig. 2a, b). Most are mRNA but 1% are non-coding RNA. Among 2,536 transcripts identified in RIP-seq, 50% overlap with PAR-CLIP targets (Extended Data Fig. 2b). We also performed m^{6}A-seq for the poly(A)-tailed RNA from the same HeLa cell line and found that 59% (7,345 out of 12,442) of the PAR-CLIP peaks of YTHDF2 overlap with m^{6}A peaks (Fig. 1c). As shown in Fig. 1d, the conserved motif revealed from the top 1,000 scored clusters matches the m^{6}A consensus sequence of RRACH[12,14], which strongly supports the binding of m^{6}A by YTHDF2 inside cells (see more motifs in Extended Data Fig. 2c–e). Coinciding with the previously reported pattern of m^{6}A peaks[14,15], YTHDF2 PAR-CLIP peaks showed enrichment near the stop codon and in long exons (Extended Data Fig. 2f–h). YTHDF2 predominantly targets the stop codon region, the 3′ untranslated region (3′ UTR), and the coding region (CDS) (Fig. 1e), indicating that YTHDF2 may have a role in mRNA stability and/or translation.

To dissect the role of YTHDF2 we used ribosome profiling to assess the ribosome loading of each mRNA represented as ribosome-protected reads[21,22]. HeLa cells that were treated with YTHDF2 short interfering RNA (siRNA) (Extended Data Fig. 3a) as well as siRNA control were subsequently subjected to ribosome profiling with mRNA sequencing (mRNA-seq) performed on the same sample. Transcripts present (reads per kilobase per million reads (RPKM) >1) in both ribosome profiling and mRNA-seq samples were analysed. These transcripts were then categorized as YTHDF2 PAR-CLIP targets (3,251), common targets of PAR-CLIP and RIP (1,277), and non-targets (3,905, absent from PAR-CLIP and RIP). A significant increase of input mRNA reads for YTHDF2 targets was observed in the YTHDF2 knockdown sample compared to the control ($P < 0.001$, Mann–Whitney U-test), without a noticeable change for non-targets (Fig. 2a). However, compared with the increase in mRNA level, the differences in the ribosome-protected fraction in the knockdown sample compared to the control were small (Fig. 2b). Thus, YTHDF2 knockdown led to apparently reduced translation efficiency of its targets as a result of accumulation of non-translating mRNA (Extended Data Fig. 3b), suggesting the primary role of YTHDF2 in RNA degradation.

Next, we performed RNA lifetime profiling by collecting and analysing RNA-seq data on YTHDF2 knockdown and control samples obtained at different time points after transcription inhibition with actinomycin D. Indeed, YTHDF2 knockdown led to prolonged (~30% in average) lifetimes of its mRNA targets in comparison with non-targets (Fig. 2c). Interestingly, we found that as the number of binding sites increase the stabilization of the RNA targets caused by YTHDF2 knockdown also increase significantly[23]: more than four sites have a larger extent of stabilization upon YTDF2 knockdown than 2–4 sites, which have larger fold changes than targets with only one site (Fig. 2d and Extended Data Fig. 3c, Kruskal–Wallis test, $P < 0.0001$); however, transcripts grouped according to binding region show similar fold-change indistinguishable in statistical test (Extended Data Fig. 3c, d).

Three pools of mRNAs exist in cytoplasm as defined by their engagement in translation[24,25] (Fig. 2e): non-ribosome mRNPs (mRNA–protein particles, with sedimentation coefficients of 20S–35S in sucrose gradient), translatable mRNA pool associated with ribosomal subunits (40S–80S), and actively translating polysome (>80S). YTHDF2 was observed to be present in non-ribosome fraction (Fig. 2e). After YTHDF2 knockdown, a 21% increase of the m^{6}A/A ratio of the total mRNA was observed (Fig. 2f), confirming that the presence of YTHDF2 destabilizes the m^{6}A-containing mRNA. YTHDF2 could affect localizing m^{6}A-containing mRNA from a translatable pool to mRNPs. If so, the amount of methylated mRNA should decrease in mRNPs and

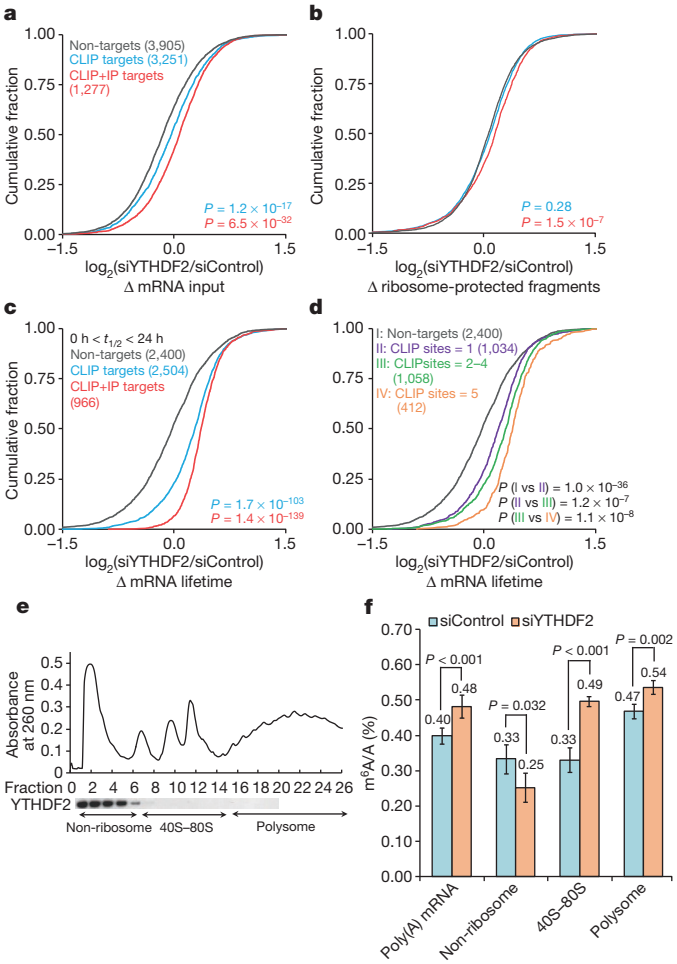

Figure 2 | YTHDF2 destabilizes its cognate mRNAs. **a**–**c**, Cumulative distribution of mRNA input (**a**), ribosome-protected fragments (**b**), and mRNA lifetime $\log_2$ fold changes (Δ, **c**) between siYTHDF2 (YTHDF2 knockdown) and siControl (knockdown control) for non-targets (grey), PAR-CLIP targets (blue), and common targets of PAR-CLIP and RIP (red). **d**, The mRNA lifetime $\log_2$ fold changes were further grouped and analysed on the basis of the number of CLIP sites on each transcript. The increased binding of YTHDF2 on its target transcript correlates with reduced mRNA lifetime. P values were calculated using two-sided Mann–Whitney or Kruskal–Wallis test (rank-sum test for the comparison of two or multiple samples, respectively). Detailed statistics are presented in Extended Data Fig. 3c. **e**, Western blotting of Flag-tagged YTHDF2 on each fraction of 10–50% sucrose gradient showing that YTHDF2 does not associate with ribosome. The fractions were grouped to non-ribosome mRNPs, 40S–80S, and polysome. **f**, Quantification of the m^{6}A/A ratio of the total mRNA, non-ribosome portion, 40S–80S, and polysome by LC-MS/MS. Noticeable increases of the m^{6}A/A ratio of the total mRNA, mRNA from 40S–80S, and mRNA from polysome were observed in the siYTHDF2 sample compared to control after 48 h. A reduced m^{6}A/A ratio of mRNA isolated from the non-ribosome portion was observed in the same experiment. P values were determined using two-sided Student's t-test for paired samples. Error bars, mean ± s.d., for poly(A)-tailed total mRNA input, $n = 10$ (five biological replicates × two technical replicates), and for the rest, $n = 4$ (two biological replicates × two technical replicates).

increase in the translatable pool upon YTHDF2 knockdown. Indeed, after YTHDF2 knockdown, the m^{6}A/A ratio of mRNA isolated from mRNPs showed a 24% decrease and the ratio from the translatable pool demonstrated a 46% increase (Fig. 2f). We also observed a 14% increase of the m^{6}A/A ratio of mRNA isolated from polysome after YTHDF2 knockdown (Fig. 2f), although it is worth noting that this model provided no prediction of the behaviour of polysome because the ribosome-loading number per transcript depends on the availability of both mRNA and free ribosomes. It should be also noted that the

observed m^{6}A/A ratio change does not seem to result from the protein level change of methyltransferase and demethylase as detected by western blotting (Extended Data Fig. 3e).

Three YTHDF2-targeted RNAs were selected for further validation: the *SON* mRNA has multiple CLIP peaks in CDS, the *CREBBP* mRNA has CLIP peaks at 3′ UTR, and a non-coding RNA *PLAC2* (Extended Data Fig. 4a–d). As detected by gene-specific PCR with reverse transcription (RT–PCR), after 48 h YTHDF2 knockdown, all three RNA transcripts increased by more than 60% with prolonged lifetime; both *SON* and *CREBBP* showed redistribution from non-ribosome mRNP to translatable pool (Extended Data Fig. 4e–n). Furthermore, knockdown of the known m^{6}A methyltransferase *MT-A70* led to noticeably reduced binding of YTHDF2 to its targets and increased stability of the targets similar to that of the YTHDF2 knockdown (Extended Data Fig. 5).

To gain mechanistic understanding of the YTHDF2–mRNA interaction, we analysed the cellular distribution of YTHDF2 and found that YTHDF2 co-localizes with three markers (DCP1a, GW182 and DDX6) of processing bodies (P bodies) in the cytoplasm, where mRNA decay occurs (Extended Data Fig. 6a–j)[9,26]. YTHDF2 is composed of a C-terminal RNA-binding domain (C-YTHDF2) and a P/Q/N-rich N terminus (N-YTHDF2, Fig. 3a and Extended Data Fig. 6k)[27,28]. Whereas overexpression of YTHDF2 led to a reduced m^{6}A/A ratio of the total mRNA, overexpression of either N-YTHDF2 or C-YTHDF2 yielded an increased m^{6}A/A ratio (Fig. 3b), indicating that both domains are required for the YTHDF2-mediated mRNA decay. An *in vitro* pull-down experiment further showed that purified C-YTHDF2 is able to enrich m^{6}A-containing mRNA from total mRNA (Extended Data Fig. 6l). The spatial distribution of the *SON* mRNA relative to YTHDF2 and N- and C-YTHDF2 truncates were examined by fluorescence *in situ* hybridization (FISH) and fluorescence immunostaining in HeLa cells (Fig. 3c–e). The location of the *SON* mRNA showed a strong correlation with that of the full-length YTHDF2 (Fig. 3c) and C-YTHDF2 (Fig. 3e). In contrast, a much lower correlation was observed for the *SON* mRNA with N-YTHDF2 (Fig. 3d). In addition, the full-length YTHDF2 and N-YTHDF2 co-localized with DCP1a, but to a much lesser extent for C-YTHDF2, thereby indicating the role of N-YTHDF2 in P-body localization. Furthermore, the overexpression of C-YTHDF2 led to a reduced co-localization of the *SON* mRNA with DCP1a (Fig. 3e).

In further support of this mechanism, N-YTHDF2 was fused with λ peptide (N-YTHDF2–λ), which recognizes Box B RNA with a high affinity in a tether reporter assay[29,30]. Tethering N-YTHDF2–λ to F-luc-5BoxB (five Box B sequence was inserted into the 3′ UTR of the mRNA reporter) led to a significantly reduced mRNA level (Fig. 3f) and shortening (40%) of its lifetime compared with tethering controls of N-YTHDF2 or λ alone (Extended Data Fig. 7a–e). The reporter mRNA bound by N-YTHDF2–λ possesses shorter poly(A) tail length in comparison with unbound portion, although a significant change of the deadenylation rate was not observed(Extended Data Fig. 7f–l). Together with the observation that YTHDF2 co-localizes with both deadenylation and decapping enzyme complexes (Extended Data Fig. 6), we propose a model (Fig. 3g) that consists of: (1) C-YTHDF2 selectively recognizes m^{6}A-containing mRNA less engaged with translation; (2) this binding of YTHDF2 to methylated mRNA happens in parallel or at a later stage of deadenylation; (3) N-YTHDF2 localizes the YTHDF2–m^{6}A-mRNA complex to more specialized mRNA decay machineries (P bodies etc.) for committed degradation.

Functional clustering of YTHDF2 targets versus non-targets revealed that the main functions of YTHDF2-mediated RNA processing are gene expression (molecular function) as well as cell death and survival (cellular function, Extended Data Fig. 8a–d). After 72 h of YTHDF2 knockdown, the viability of HeLa cells reduced by 50% (Extended Data Fig. 8e, f), indicating that the YTHDF2-mediated RNA processing could have biological significance.

In summary, we present a transcriptome-wide identification of YTHDF2–RNA interaction and a mechanistic model for m^{6}A function

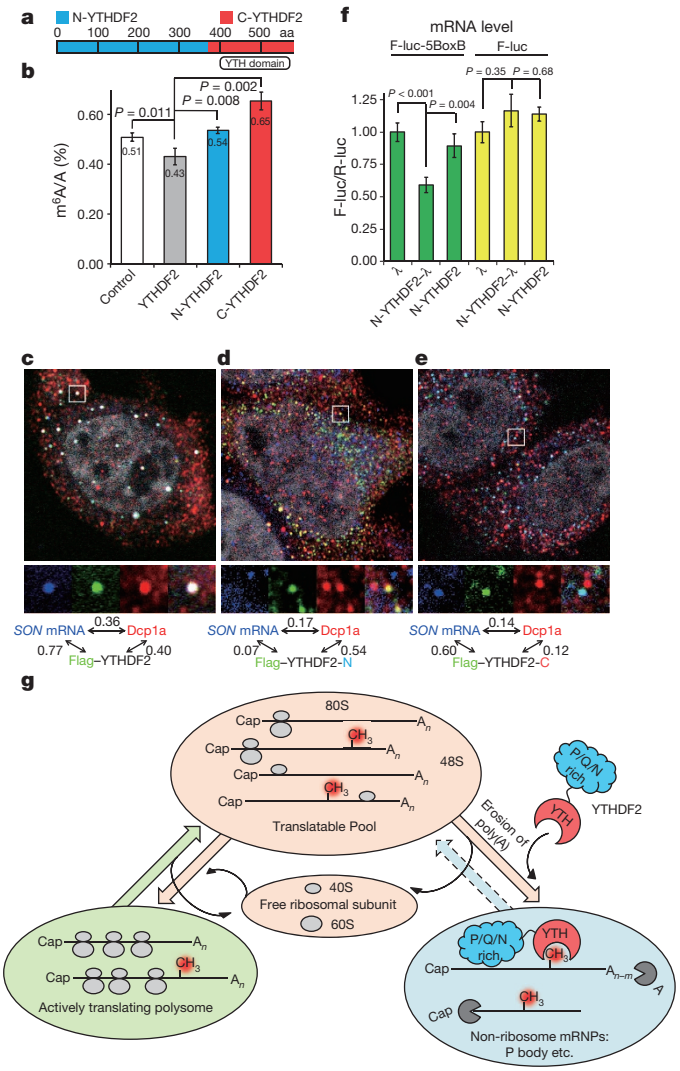

Figure 3 | YTHDF2 affects *SON* mRNA localization in processing body (P-body). **a**, Schematic of the domain architecture (aa, amino acids) of YTHDF2, N terminus of YTHDF2 (N-YTHDF2, aa 1–389, blue) and C terminus of YTHDF2 (C-YTHDF2, aa 390–end, red). **b**, Overexpression of full-length YTHDF2 led to reduced levels of m^{6}A after 24 h, whereas overexpression of N-YTHDF2 or C-YTHDF2 increased the m^{6}A/A ratio of the total mRNA. *P* values were determined using two-sided Student's *t*-test for paired samples. Error bars, mean ± s.d., $n = 4$ (two biological replicates × two technical replicates). **c**–**e**, Fluorescence *in situ* hybridization of *SON* mRNA and fluorescence immunostaining of DCP1a (P-body marker), Flag-tagged YTHDF2 (**c**), Flag-tagged C-YTHDF2 (**d**), and Flag-tagged N-YTHDF2 (**e**). Full-length YTHDF2 and C-YTHDF2 co-localize with *SON* mRNA (bearing m^{6}A) and the full-length YTHDF2 significantly increases the P-body localization of *SON* mRNA compared to N-YTHDF2 and C-YTDF2. The numbers shown above figures are Pearson correlation coefficients of each channel pair with the scale of the magnified region (white frame) set as 2 μm × 2 μm. **f**, Tethering N-YTHDF2–λ to a mRNA reporter F-luc-5BoxB led to a ~40% reduction of the reporter mRNA level compared to tethering N-YTHDF2 or λ alone (green) and controls without BoxB (F-luc, yellow). *P* values were determined using two-sided Student's *t*-test for paired samples. Error bars, mean ± s.d., $n = 6$ (F-luc-5BoxB) or 3 (F-luc). **g**, A proposed model of m^{6}A-dependent mRNA degradation mediated through YTHDF2. The three states of mRNAs in cytoplasm are defined by their engagement with ribosome using the sedimentation coefficient range in sucrose gradient: >80S for actively translating polysome; 40S–80S for translatable pool; 20S–35S for non-ribosome mRNPs.

mediated by this m^{6}A-binding protein, as the first functional demonstration of a m^{6}A reader protein. We show that YTHDF2 alters the distribution of the cytoplasmic states of several thousand m^{6}A-containing

mRNA. This present work demonstrates that reversible m^{6}A deposition could dynamically tune the stability and localization of the target RNAs through m^{6}A 'readers'.

METHODS SUMMARY

m^{6}A profiling, PAR-CLIP and RIP experiments were conducted as previously reported[14,19,20]. For ribosome profiling, RPF was obtained by micrococcal nuclease digestion followed by sucrose gradient (10–50%) separation. Complementary DNA libraries of RPF and mRNA input were constructed as previously described[22]. In RNA lifetime profiling, actinomycin D (5 μg ml^{-1}) was added to stop transcription, and samples at 0, 3 and 6 h decay were collected. ERCC RNA spike-in control (Ambion) was added to each sample before the isolation of mRNA and library construction to correct the decrease of the whole mRNA population during RNA decay. All of the cDNA libraries were sequenced by using Hiseq 2000 (Illumina, single end, 100 bp) and at least two replicates were performed for each experiment (Extended Data Table 1). The deep sequencing data were mapped to Human genome version hg19 without any gaps and allowed for at most two mismatches. The PAR-CLIP binding sites were identified through kernel density estimation of T to C conversions. For RIP, transcripts that have more than twofold enrichment were identified as targets. For ribosome profiling and mRNA lifetime profiling, the average of the $\log_2$(siYTHDF2/siControl) values generated from two biological replicates were analysed and comparisons of independent replicates were summarized in Extended Data Fig. 9.

Online Content Any additional Methods, Extended Data display items and Source Data are available in the online version of the paper; references unique to these sections appear only in the online paper.

Received 31 December 2012; accepted 3 October 2013.

Published online 27 November 2013; corrected online 1 January 2014 (see full-text HTML version for details).

1. Tuck, M. T. The formation of internal 6-methyladenine residues in eucaryotic messenger RNA. *Int. J. Biochem.* **24,** 379–386 (1992).
2. Jia, G., Fu, Y. & He, C. Reversible RNA adenosine methylation in biological regulation. *Trends Genet.* **29,** 108–115 (2013).
3. Clancy, M. J., Shambaugh, M. E., Timpte, C. S. & Bokar, J. A. Induction of sporulation in *Saccharomyces cerevisiae* leads to the formation of N^6-methyladenosine in mRNA: a potential mechanism for the activity of the *IME4* gene. *Nucleic Acids Res.* **30,** 4509–4518 (2002).
4. Zhong, S. *et al.* MTA is an *Arabidopsis* messenger RNA adenosine methylase and interacts with a homolog of a sex-specific splicing factor. *Plant Cell* **20,** 1278–1288 (2008).
5. Hongay, C. F. & Orr-Weaver, T. L. *Drosophila* Inducer of MEiosis 4 (IME4) is required for Notch signaling during oogenesis. *Proc. Natl Acad. Sci. USA* **108,** 14855–14860 (2011).
6. Frayling, T. M. *et al.* A common variant in the *FTO* gene is associated with body mass index and predisposes to childhood and adult obesity. *Science* **316,** 889–894 (2007).
7. Jia, G. *et al.* N^6-methyladenosine in nuclear RNA is a major substrate of the obesity-associated FTO. *Nature Chem. Biol.* **7,** 885–887 (2011).
8. Zheng, G. *et al.* ALKBH5 is a mammalian RNA demethylase that impacts RNA metabolism and mouse fertility. *Mol. Cell* **49,** 18–29 (2013).
9. Sheth, U. & Parker, R. Decapping and decay of messenger RNA occur in cytoplasmic processing bodies. *Science* **300,** 805–808 (2003).
10. Dandekar, T. & Bengert, P. *RNA Motifs and Regulatory Elements* 2nd edn, 1–11, (Springer, 2002).
11. He, C. Grand challenge commentary: RNA epigenetics? *Nature Chem. Biol.* **6,** 863–865 (2010).
12. Wei, C. M. & Moss, B. Nucleotide sequences at the N^6-methyladenosine sites of HeLa cell messenger ribonucleic acid. *Biochemistry* **16,** 1672–1676 (1977).
13. Bokar, J. A., Shambaugh, M. E., Polayes, D., Matera, A. G. & Rottman, F. M. Purification and cDNA cloning of the AdoMet-binding subunit of the human mRNA (N^6-adenosine)-methyltransferase. *RNA* **3,** 1233–1247 (1997).
14. Dominissini, D. *et al.* Topology of the human and mouse m^{6}A RNA methylomes revealed by m^{6}A-seq. *Nature* **485,** 201–206 (2012).
15. Meyer, K. D. *et al.* Comprehensive analysis of mRNA methylation reveals enrichment in 3′ UTRs and near stop codons. *Cell* **149,** 1635–1646 (2012).
16. Stoilov, P., Rafalska, I. & Stamm, S. YTH: a new domain in nuclear proteins. *Trends Biochem. Sci.* **27,** 495–497 (2002).
17. Zhang, Z. *et al.* The YTH domain is a novel RNA binding domain. *J. Biol. Chem.* **285,** 14701–14710 (2010).
18. Cardelli, M. *et al.* A polymorphism of the *YTHDF2* gene (1p35) located in an Alu-rich genomic domain is associated with human longevity. *J. Gerontol. A* **61,** 547–556 (2006).
19. Hafner, M. *et al.* Transcriptome-wide identification of RNA-binding protein and microRNA target sites by PAR-CLIP. *Cell* **141,** 129–141 (2010).
20. Peritz, T. *et al.* Immunoprecipitation of mRNA-protein complexes. *Nature Protocols* **1,** 577–580 (2006).
21. Ingolia, N. T., Ghaemmaghami, S., Newman, J. R. & Weissman, J. S. Genome-wide analysis *in vivo* of translation with nucleotide resolution using ribosome profiling. *Science* **324,** 218–223 (2009).
22. Bazzini, A. A., Lee, M. T. & Giraldez, A. J. Ribosome profiling shows that miR-430 reduces translation before causing mRNA decay in zebrafish. *Science* **336,** 233–237 (2012).
23. Mukherjee, N. *et al.* Integrative regulatory mapping indicates that the RNA-binding protein HuR couples pre-mRNA processing and mRNA stability. *Mol. Cell* **43,** 327–339 (2011).
24. Huang, R., Brown, C. Y. & Morris, D. R. In *mRNA Formation and Function* (ed. Richter, J. D.) Ch. 16 (Academic Press, 1997).
25. Shenton, D. *et al.* Global translational responses to oxidative stress impact upon multiple levels of protein synthesis. *J. Biol. Chem.* **281,** 29011–29021 (2006).
26. Kedersha, N. & Anderson, P. Mammalian stress granules and processing bodies. *Methods Enzymol.* **431,** 61–81 (2007).
27. Reijns, M. A., Alexander, R. D., Spiller, M. P. & Beggs, J. D. A role for Q/N-rich aggregation-prone regions in P-body localization. *J. Cell Sci.* **121,** 2463–2472 (2008).
28. Kato, M. *et al.* Cell-free formation of RNA granules: low complexity sequence domains form dynamic fibers within hydrogels. *Cell* **149,** 753–767 (2012).
29. Gehring, N. H., Neu-Yilik, G., Schell, T., Hentze, M. W. & Kulozik, A. E. Y14 and hUpf3b form an NMD-activating complex. *Mol. Cell* **11,** 939–949 (2003).
30. Behm-Ansmant, I. *et al.* mRNA degradation by miRNAs and GW182 requires both CCR4:NOT deadenylase and DCP1:DCP2 decapping complexes. *Genes Dev.* **20,** 1885–1898 (2006).

Acknowledgements This work is supported by National Institutes of Health GM071440 (C.H.) and EUREKA GM088599 (T.P. and C.H.). The Mass Spectrometry Facility of the University of Chicago is funded by National Science Foundation (CHE-1048528). We thank A. E. Kulozik, W. Filipowicz and J. A. Steitz for providing the sequence and plasmids of the tether reporter. We thank Dr. G. Zheng and W. Clark for help in polysome profiling. We also thank S. F. Reichard for editing the manuscript.

Author Contributions C.H. conceived the project. X.W. designed and performed most experiments. Z.L. and X.W. performed data analyses of high-throughput sequencing data. A.G. assisted with the experiments. Y.Y. and D.H. conducted the experimental and data analysis part of m^{6}A profiling, respectively. Y.F. performed the RNA-affinity pull-down experiment of YTHDF1 and YTHDF3. M.P. and G.J. provided valuable discussions. G.C.H. and B.R. performed high throughput sequencing. Q.D. assisted in m^{6}A synthesis. X.W. and C.H. interpreted the results and wrote the manuscript with input from T.P.

Author Information RNA sequencing data were deposited in the Gene Expression Omnibus (http://www.ncbi.nlm.nih.gov/geo) under accession number GSE49339 and the processed results were presented as Supplementary Table 1. Processed files were deposited in the Gene Expression Omnibus under accession no. GSE46705. Reprints and permissions information is available at www.nature.com/reprints. The authors declare no competing financial interests. Readers are welcome to comment on the online version of the paper. Correspondence and requests for materials should be addressed to C.H. (chuanhe@uchicago.edu).

METHODS

Plasmid construction and protein expression. Recombinant YTHDF1-3 were cloned from commercial cDNA clones (Open Biosystems) into vector pGEX-4T-1. The primers used for subcloning (from 5′ to 3′; F stands for forward primer; R stands for reverse primer) are listed: GST-YTHDF1-F, CGATCGAATTCATG TCGGCCACCAGCG; GST-YTHDF1-R, CCATACTCGAGTCATTGTTTGTTT CGACTCTGCC; GST-YTHDF2-F, CGTACGGATCCATGTCAGATTCCTACT TACCCAG; GST-YTHDF2-R, CGATGCTCGAGTCATTTCCCACGACCTTG ACG; GST-YTHDF3-F, CGTACGGATCCATGTCAGCCACTAGCGTG; GST-YTHDF3-R, CGTAGCTCGAGTCATTGTTTGTTTCTATTTCTCTCCCTAC.

The resulting clones were transfected into the *Escherichia coli* strain BL21 and expression was induced at 16 °C with 1 mM IPTG for 20 h. The pellet collected from 2 litres of bacteria culture was then lysed in 30 ml PBS-L solution (50 mM NaH_2PO_4, 150 mM NaCl, pH 7.2, 1 mM PMSF, 1 mM DTT, 1 mM EDTA, 0.1% (v/v) Triton X-100) and sonicated for 10 min. After removing cell debris by centrifuge at 17,000*g* for 30 min, the supernatant were loaded to a GST superflow cartridge (Qiagen, 5 ml) and gradiently eluted by using PBS-EW (50 mM NaH_2PO_4, 150 mM NaCl, pH 7.2,1 mM DTT, 1 mM EDTA) as buffer A and TNGT (50 mM Tris, pH 8.0, 150 mM NaCl, 50 mM red, GSH, 0.05% Triton X-100) as buffer B. The crude products were further purified by gel-filtration chromatography in GF buffer (10 mM Tris, pH 7.5, 200 mM NaCl, 3 mM DTT and 5% glycerol). The yield was around 1–2 mg per litre of bacterial culture.

Flag-tagged YTHDF2 was cloned into vector pcDNA 3.0 (BamHI, XhoI, forward primer, CGTACGGATCCATGGATTACAAGGACGACGATGACAAGA TGTCGGCCAGCAGCC; reverse primer, CGATGCTCGAGTCATTTCCCACG ACCTTGACG). Flag-tagged YTHDF2 N-terminal domain was made by mutating E384 (GAA) to a stop codon (TAA) with a Stratagene QuikChange II site-directed mutagenesis kit (pcDNA-Flag-Y2N, forward primer, CTGGATCTACTCCTTCATAA CCCCACCCAGTGTTG; reverse primer, CAACACTGG GTGGGGTTATGAA GGAGTAGATCCAG). Flag-tagged YTHDF2 C-terminal domain was made by cloning amino acids from E384 to the end into vector pcDNA 3.0 (BamHI, XhoI, forward primer, CGTACGGATCCATGGATTACAAGGACGACGATGACAA GGAACCCCACCC AGTGTT; reverse primer, CGATGCTCGAGTCATTTCCC ACGACCTTGACG). Plasmids with high purity for mammalian cell transfection were prepared with a Maxiprep kit (Qiagen).

Tether reporter: pmirGlo Dual luciferase expression vector (Promega) was used to construct the tether reporter which contains firefly luciferase (F-luc) as the primary reporter and *Renilla* luciferase (R-luc) acting as a control reporter for normalization. F-luc-5BoxB mRNA reporter was obtained by inserting five Box B sequence (5BoxB) into the 3′ UTR of F-luc (SacI and XhoI, the resulting plasmid was named as pmirGlo-5BoxB;). The 5BoxB sequence[29] (see below) was PCR-amplified from PRL-5BoxB plasmid, which was provided by W. Filipowi (forward primer, CGATACGAGCTCTTCCCTAAGTCCAACTACCAAAC; reverse primer, CTATGGCTCGAGATAATATCCTCGATAGGGCCC; sequencing primer, GACGAGGTGCCTAAAGA)[31].

The 5BoxB sequence: TTCCCTAAGTCCAACTACTAAACTGGGGATTCCT GGGCCCTGAAGAAGGGCCCCTCGACTAAGTCCAACTACTAAACTGGGC CCTGAAGAAGGGCCCATATAGGGCCCTGAAGAAGGGCCCTATCGAGG ATATTATCTCGACTAAGTCCAACTACTAAACTGGGCCCTGAAGAAGGG CCCATATAGGGCCCTGAAGAAGGGCCCTATCGAGGATATTATCTCGAG.

To study the decay kinetics of F-luc-5BoxB, another reporter plasmid (pmirGlo-Ptight-5BoxB) was constructed by replacing the original human phosphoglycerate kinase promoter of F-luc with Ptight promoter (restriction sites: ApaI and BglII). Ptight promoter was PCR amplified from pTRE-Tight vector (Clontech; forward primer, CGTACAGATCTCGAGTTTACTCCCTATCAGT; reverse primer, CTG TAGGGCCCT TCTTAATGTTTTTGGCATCTTCCATCTCCAGGCGATCTG ACG; sequencing primer, AGCGGTGCGTACAATTAAGG). The resulting plasmid (pmirGlo-Ptight) was subjected to a second round of subcloning by inserting 5BoxB into the 3′ UTR of F-luc (restriction sites: XbaI and SbfI) to generate pmirGlo-Ptight-5BoxB (forward primer, CGATACTCTAGATTCCCTAAGTCC AACTACCAAAC; reverse primer, CTATGGCCTGCAGGATAATATCCTCG ATAGGGCCC; sequencing primer, GACGAGGTGCCTAA AGA).

Tether effecter: λ peptide sequence (MDAQTRRRERRAEKQAQWKAAN) was fused to the C terminus of N-YTHDF2 by subcloning N-YTHDF2 to pcDNA 3.0 with forward primer containing Flag-tag sequence and reverse primer containing λ peptide sequence (pcDNA-Flag-Y2Nλ, BamHI, XhoI; forward primer, GATACGG ATCCATGGATTACAAGGACGACGATGACAAGATGTCGGCCAGCAGCC; reverse primer, TATGGCTCGAGTCAGTTTGCAGCTTTCCATTGAGCTTGT TTCTCAGCGCGACGCTCACGTCGTCGTGTTTGTGCGTCCATACCTGAA GGAGTAGATCCAGAACC). The λ peptide control was designed with a Flag tag at N-terminal and a GGS spacer (pcDNA-Flag-λ). The primer pair that contains Flag-tagged λ peptide and sticky restriction enzyme sites (*BamH*I, *Xho*I) was annealed and directly ligated to digested pcDNA 3.0 (forward primer, GAT CCATGGATTACAAGGACGACGATGACAAGGGTGGTAGCATGGACGCA CAAACACGACGACGTGAGCGTCGCGCTGAGAAACAAGCTCAATGGAA AGCTGCAAACTAAC; reverse primer, GAGTTAGTTTGCAGCTTTCCATTG AGCTTGTTTCTCAGCGCGACGCTCACGTCGTCGTGTTTGTGCGTCCATG CTACCACCCTTGTCATCGTCGTCCTTGTAATCCATG).

EMSA (electrophoretic mobility shift assay/gel shift assay). The RNA probe was synthesized by a previously reported method with the sequence of 5′-AUGGGC CGUUCAUCUGCUAAAAGGXCUGCUUUUGGGGCUUGU-3′ (X = A or m^6A). After the synthesis, the RNA probe was labelled in a reaction mixture of 2 μl RNA probe (1 μM), 5 μl 5 × T4 PNK buffer A (Fermentas), 1 μl T4 PNK (Fermentas), 1 μl [^{32}P]ATP and 41 μl RNase-free water (final RNA concentration 40 nM) at 37 °C for 1 h. The mixture was then purified by RNase-free micro bio-spin columns with bio-gel P30 in Tris buffer (Bio-Rad 732-6250) to remove hot ATP and other small molecules. To the elute, 2.5 μl 20 × SSC (Promega) buffer was added. The mixture was heated to 65 °C for 10 min to denature the RNA probe, and then slowly cooled down to room temperature. GST–YTHDF1, GST–YTHDF2 and GST–YTHDF3 were diluted to concentration series of 200 nmol, 1 μM, 5 μM, 20 μM and 100 μM (or other indicated concentrations) in binding buffer (10 mM HEPES, pH 8.0, 50 mM KCl, 1 mM EDTA, 0.05% Triton-X-100, 5% glycerol, 10 μg ml^{-1} salmon DNA, 1 mM DTT and 40 U ml^{-1} RNasin). Before loading to each well, 1 μl RNA probe (4 nM final concentration) and 1 μl protein (20 nM, 100 nM, 500 nM, 2 μM or 10 μM final concentration) were added and the solution was incubated on ice for 30 min. The entire 10 μl RNA–protein mixture was loaded to the gel (Novex 4∼20% TBE gel) and run at 4 °C for 90 min at 90 V. Quantification of each band was carried out by using a storage phosphor screen (K-Screen; Fuji film) and Bio-Rad Molecular Imager FX in combination with Quantity One software (Bio-Rad). The K_d (dissociation constant) was calculated with nonlinear curve fitting (Function Hyperbl) of Origin 8 software with $y = P_1 \times x/(P_2 + x)$, where y is the ratio of [RNA–protein]/[free RNA]+[RNA–protein], x is the concentration of the protein, P_1 is set to 1 and P_2 is K_d.

Mammalian cell culture, siRNA knockdown and plasmid transfection. Human HeLa cell line used in this study was purchased from ATCC (CCL-2) and grown in DMEM (Gibco, 11965) media supplemented with 10% FBS and 1% 100 × Pen Strep (Gibco). HeLa Tet-off cell line was purchased from Clontech and grown in DMEM (Gibco) media supplemented with 10% FBS (Tet system approved, Clontech), 1% 100 × Pen Strep (Gibco) and 200 μg ml^{-1} G418 (Clontech). AllStars negative control siRNA from Qiagen (1027281) was used as control siRNA in knockdown experiments. *YTHDF2* siRNA was ordered from Qiagen as custom synthesis which targets 5′-AAGGACGTTCCCAATAGCCAA-3′ near the N terminus of CDS. *MT-A70* siRNA was ordered from Qiagen: 5′-CGTCAGTATCTTGGGCAAGTT-3′. Transfection was achieved by using Lipofectamine RNAiMAX (Invitrogen) for siRNA, and Lipofectamine 2000 for single type of plasmid or Lipofectamine LTX Plus (Invitrogen) for co-transfection of two or multiple types of plasmids (tethering assay) following the manufacturer's protocols.

RNA isolation. mRNA isolation for LC-MS/MS: total RNA was isolated from wild-type or transiently transfected cells with TRIzol reagent (Invitrogen). mRNA was extracted using PolyATtract mRNA Isolation Systems IV (Promega) followed by further removal of contaminated rRNA by using RiboMinus Transcriptome Isolation Kit (Invitrogen). mRNA concentration was measured by NanoDrop. Total RNA isolation for RT–PCR: following the instruction of RNeasy kit (Qiagen) in addition to DNase I digestion step. Ethanol precipitation: to the RNA solution being purified or concentrated, 1/10 volume of 3 M NaOAc, pH 5.5, 1 μl glycogen (10 mg ml^{-1}) and 2.7 volume of 100% ethanol were added, stored at −80 °C for 1 h to overnight, and then centrifuged at 15,000*g* for 15 min. After the supernatant was removed, the pellet was washed twice by using 1 ml 75% ethanol, and dissolved in the appropriate amount of RNase-free water as indicated.

***In vitro* pull down.** 0.8 μg mRNA (save 0.2 μg from the same sample as input) and YTHDF1, YTHDF2, YTHDF3 or C-YTHDF2 (final concentration 500 nM) were diluted into 200 μl IPP buffer (150 mM NaCl, 0.1% NP-40, 10 mM Tris, pH 7.4, 40 U ml^{-1} RNase inhibitor, 0.5 mM DTT), and the solution was mixed with rotation at 4 °C for 2 h. For YTHDF1, YTHDF2, YTHDF3, 10 μl GST-affinity magnetic beads (Pierce) were used for each sample after being washed four times with 200 μl IPP buffer for each wash. For C-YTHDF2, 20 μl Dynabeads His-Tag Isolation & Pulldown beads (Invitrogen) were used after being washed four times with 200 μl IPP buffer for each wash. The beads were then re-suspended in 50 μl IPP buffer. The protein–RNA mixture was combined with GST or His6 beads and kept rotating for another 2 h at 4 °C. The aqueous phase was collected, recovered by ethanol precipitation, dissolved in 15 μl water, and saved as the flow-through. The beads were washed four times with 300 μl IPP buffer each time. 0.4 ml TRIzol reagent was added to the beads and further purified according to the manufacturer's instructions. The purified fraction was dissolved in 15 μl water, and saved as YTHDF-bound. LC-MS/MS was used to measure the level of m^6A in each sample of input, flow-through and YTHDF-bound.

LC-MS/MS[7,8]. 200–300 ng of mRNA was digested by nuclease P1 (2 U) in 25 μl of buffer containing 25 mM of NaCl, and 2.5 mM of $ZnCl_2$ at 37 °C for 2 h, followed by the addition of NH_4HCO_3 (1 M, 3 μl) and alkaline phosphatase (0.5 U). After an additional incubation at 37 °C for 2 h, the sample was diluted to 50 μl and filtered (0.22 μm pore size, 4 mm diameter, Millipore), and 5 μl of the solution was injected into LC-MS/MS. Nucleosides were separated by reverse phase ultra-performance liquid chromatography on a C18 column with on-line mass spectrometry detection using an Agilent 6410 QQQ triple-quadrupole LC mass spectrometer in positive electrospray ionization mode. The nucleosides were quantified by using the nucleoside to base ion mass transitions of 282 to 150 (m^6A), and 268 to 136 (A). Quantification was performed in comparison with the standard curve obtained from pure nucleoside standards running on the same batch of samples. The ratio of m^6A to A was calculated based on the calibrated concentrations.

m^6A profiling. Total RNA was isolated from HeLa cells with TRIzol reagent. Poly(A)$^+$ RNA was further enriched from total RNA by using FastTrack MAG Maxi mRNA isolation kit (Invitrogen). In particularly, an additional DNase I digestion step was applied to all the samples to avoid DNA contamination. RNA fragmentation, m^6A-seq, and library preparation were performed according to the previous protocol developed in ref. 14. The experiment was conducted in two biological replicates (Extended Data Table 1).

RIP-seq. The procedure was adapted from the previous report[20]. 60 million HeLa cells were collected (three 15-cm plates, after 24 h transfection of Flag-tagged YTHDF2) by cell lifter (Corning Incorporated), pelleted by centrifuge for 5 min at 1,000*g* and washed once with cold PBS (6 ml). The cell pellet was re-suspended with 2 volumes of lysis buffer (150 mM KCl, 10 mM HEPES pH 7.6, 2 mM EDTA, 0.5% NP-40, 0.5 mM DTT, 1:100 protease inhibitor cocktail, 400 U ml^{-1} RNase inhibitor; one plate with ~200 μl cell pellet and ~400 μl lysis buffer), pipetted up and down several times, and then the mRNP lysate was incubated on ice for 5 min and shock-frozen at −80 °C with liquid nitrogen. The mRNP lysate was thawed on ice and centrifuged at 15,000*g* for 15 min to clear the lysate. The lysate was further cleared by filtering through a 0.22 μm membrane syringe. 50 μl cell lysate was saved as input, mixed with 1 ml TRIzol. The anti-Flag M2 magnetic beads (Sigma, 20 μl per ml lysate, ~30 μl to each sample) was washed with a 600 μl NT2 buffer (200 mM NaCl, 50 mM HEPES pH 7.6, 2 mM EDTA, 0.05% NP-40, 0.5 mM DTT, 200 U ml^{-1} RNase inhibitor) four times and then re-suspended in 800 μl ice-cold NT2 buffer. Cell lysate was mixed with M2 beads; the tube was flicked several times to mix the contents and then rotated continuously at 4 °C for 4 h. The beads were collected, washed eight times with 1 ml ice-cold NT2 buffer. 5 packed beads volumes (~150 μl = 30 μl × 5) of elution solution which was 500 ng μl^{-1} 3 × Flag peptide (Sigma) in NT2 buffer were added to each sample, and the mixture was rotated at 4 °C for 2 h to elute. The supernatant was mixed with 1 ml TRIzol and saved as IP. RNA recovered from input was further subjected to mRNA purification by either Poly(A) selection (replicate 1, FastTrack MAG Micro mRNA isolation kit, invitrogen) or rRNA removal (replicate 2, RiboMinus Eukaryote Kit v2, Ambion). Input mRNA and IP with 150-200 ng RNA of each sample were used to generate the library using TruSeq stranded mRNA sample preparation kit (Illumina).

PAR-CLIP. We followed the previously reported protocol[32] with the following modifications. Sample preparation: Five 15-cm plates of HeLa cells were seeded at Day 1 18:00. At Day 2 10:00, the HeLa cells were transfected with Flag-tagged YTHDF2 plasmid at 80% confluency. After six hours, the media was changed and 200 μM 4SU was added. At Day 3 10:00, the media was aspirated, and the cells were washed once with 5 ml ice-cold PBS for each plate. The plates were kept on ice, and the crosslink was carried out by 0.15 J cm^{-2} Ultraviolet light. 2 ml PBS was added and the cells were collected by cell lifter.

Library construction: the final recovered RNA sample was further cleaned by RNA Clean & Concentrator (Zymo Research) before library construction by Truseq small RNA sample preparation kit (Illumina).

Mild enzyme digestion[33]: The first round of T1 digest was carried out under 0.2 U μl^{-1} for 15 min instead of 1 U μl^{-1} for 15 min. The second round of T1 digest was conducted under 10 U μl^{-1} for 8 min instead of 50 U μl^{-1} for 15 min.

Ribosome and polysome profiling. The procedure was adapted from the previous report[22]. Eight 15-cm plates of HeLa cells were prepared for 48 h knockdown (siControl, siYTHDF2, four plates each). Before collection, cycloheximide (CHX) was added to the media at 100 μg ml^{-1} for 7 min. The media was removed, and the cells were collected by cell lifter with 5 ml cold PBS with CHX (100 μg ml^{-1}). The cell suspension was spun at 400*g* for 2 min and the cell pellet was washed once by 5 ml PBS-CHX per plate. 1 ml lysis buffer (10 mM Tris, pH 7.4, 150 mM KCl, 5 mM $MgCl_2$, 100 μg ml^{-1} CHX, 0.5% Triton-X-100, freshly add 1:100 protease inhibitor, 40 U ml^{-1} SUPERasin) was added to suspend the cells and then kept on ice for 15 min with occasional pipetting and rotating. After centrifugation at 15,000*g* for 15 min, the supernatant (~1.2 ml) was collected and absorbance tested at 260 nm (150–200 $A_{260\,nm}$ ml^{-1}). To the lysate, 8 μl DNase Turbo was added. The lysate was then split by the ratio of 1:4 (Portion I/Portion II). 4 μl Super RNasin was added to Portion I. 40 μl MNase buffer and 3 μl MNase (6,000 gel units, NEB) was added to Portion II. Both portions were kept at room temperature for 15 min, and then 8 μl SUPERasin was added to Portion II to stop the reaction. Portion I was saved and mixed with 1 ml TRIzol to purify input mRNA. Portion II was used for ribosome profiling.

Ribosome profiling: a 10/50% w/v sucrose gradient was prepared in a lysis buffer without Triton-X-100. Portion II was loaded onto the sucrose gradient and centrifuged at 4 °C for 4 h at 27,500 r.p.m. (Beckman, rotor SW28). The sample was then fractioned and analysed by Gradient Station (BioCamp) equipped with ECONO Uv monitor (BioRad) and fraction collector (FC203B, Gilson). The fractions corresponding to 80S monosome (not 40S or 60S) were collected, combined, and mixed with an equal volume of TRIzol to purify the RNA. The RNA pellet was dissolved in 30 μl water, mixed with 30 μl 2 × TBE-urea loading buffer (Invitrogen), and separated on a 10% TBE-urea gel. A 21-nt and a 42-nt ssRNA oligo were used as size markers, and the gel band between 21 and 42 nt was cut. The gel was passed through a needle hole to break the gel, and 600 μl extraction buffer (300 mM NaOAc, pH 5.5, 1 mM EDTA, 0.1 U ml^{-1} RNasin) was added. The gel slurry was heated at 65 °C for 10 min with shaking, and then filtered through 1 ml Qiagen filter. RNA was concentrated by ethanol precipitation and finally dissolved in 10 μl of RNase-free water.

Input mRNA: the input RNA was first purified by TRIzol and the input mRNA was then separated by PolyATract. The resulting mRNA was concentrated by ethanol precipitation and dissolved in 10 μl of RNase-free water. The mRNA was fragmented by RNA fragmentation kit (Ambion). The reaction was diluted to 20 μl and cleaned up by micro Bio-Spin 30 column (cut-off: 20 bp; exchange buffer to Tris).

Library construction: the end structures of the RNA fragments of ribosome profiling and mRNA input were repaired by T4 PNK: (1) 3′ de-phosphorylation: RNA (20 μl) was mixed with 2.5 μl PNK buffer and 1 μl T4 PNK, and kept at 37 °C for 1 h; (2) 5′-phosphorylation: to the reaction mixture, 1 μl 10 mM ATP and 1 μl extra T4 PNK were added, and the mixture was kept at 37 °C for 30 min. The RNA was purified by 500 μl TRIzol reagent, and finally dissolved in 10 μl water. The library was constructed by Tru-seq small RNA sample preparation kit (Illumina). The sequencing data obtained from ribosome profiling (portion II) were denoted as ribosome-protected fragments and that from RNA input (portion I) as mRNA input. Translation efficiency was defined as the ratio of ribosome-protected fragments and mRNA input, which reflected the relative occupancy of 80S ribosome per mRNA species.

Polysome profiling: sample preparation and sucrose gradient were the same as those of the ribosome profiling procedure except eliminating MNase digestion. The fractions resulting from sucrose gradient were used for western blotting or pooled to isolate total RNA for RT–PCR and mRNA for LC-MS/MS test of m^6A/A ratio.

RNA-seq for mRNA lifetime. Two 10-cm plates of HeLa cells were transfected with YTHDF2 siRNA or control siRNA at 30% confluency. After 6 h, each 10-cm plate was re-seeded into three 6-cm plates, and each plate was controlled to afford the same amount of cells. After 48 h, actinomycin D was added to 5 μg ml^{-1} at 6 h, 3 h, and 0 h before trypsinization collection. The total RNA was purified by RNeasy kit (Qiagen). Before construction of the library with Tru-seq mRNA sample preparation kit (Illumina), ERCC RNA spike-in control (Ambion) was added to each sample (0.1 μl per sample). Two biological replicates were generated: (1) in replicate 1, RNA spike-in control was added proportional to cell numbers; (2) in replicate 2, RNA spike-in control was added proportional to total RNA. Although data obtained from the two sets showed systematic shift, they led to consistent conclusion that YTHDF2 knockdown leads to prolonged lifetime of its RNA targets (Extended Data Fig. 9).

Data analysis of seq-data. General pre-processing of reads: All samples were sequenced by illumine Hiseq2000 with single end 100-bp read length. For libraries that generated from small RNA (PAR-CLIP and ribosome profiling), the adapters was trimmed by using FASTX-Toolkit[34]. The deep sequencing data were mapped to Human genome version hg19 by Tophat version 2.0[35] without any gaps and allowed for at most two mismatches. RIP and Ribosome profiling were analysed by DESeq[36] to generate RPKM (reads per kilobase, per million reads). mRNA lifetime data were analysed by Cuffdiff version 2.0[37] to calculate RPKM.

Data analysis for each experiment: (1) for m^6A profiling, the m^6A-enriched regions in each m^6A-immunoprecipitation sample were extracted by using the model-based analysis of ChIP-seq (MACS) peak-calling algorithm[38], with the corresponding m^6A-Input sample serving as the input control. For each library, the enriched peaks with $P < 10^{-5}$ were used for further analysis; (2) for RIP, enrichment fold was calculated as $\log_2$(IP/input); (3) PAR-CLIP data were analysed by PARalyzerv1.1 with default settings[39]; (4) for ribosome profiling, only genes with RPKM >1 were used for analysis and the change fold was calculated as $\log_2$(siYTHDF2/siControl); (5) for mRNA lifetime profiling: RKPM were converted to attomole by linear-fitting of the RNA spike-in.

The degradation rate of RNA k was estimated by

$$\log_2\left(\frac{A_t}{A_0}\right) = -kt$$

where t is transcription inhibition time (h), A_t and A_0 represent mRNA quantity (attomole) at time t and time 0. Two k values were calculated: time 3 h versus time 0 h, and time 6 h versus time 0 h. The final lifetime was calculated by using the average of $k_{3\,h}$ and $k_{6\,h}$.

$$t_{\frac{1}{2}} = \frac{2}{k_{3h} + k_{6h}}$$

Integrative data analysis and statistics: PAR-CLIP targets were defined as reproducible gene targets among three biological replicates (3,251). RIP targets (2,528) were genes with $\log_2$(IP/input) > 1. The overlap of PAR-CLIP and RIP targets were defined as CLIP+IP targets (1,277). And non-targets (3,905) should meet the conditions: (1) complementary set of PAR-CLIP targets; (2) RIP enrichment fold <0. For the comparison of PAR-CLIP and m^{6}A peaks, at least 1 bp overlap was applied as the criteria of overlap peaks. Two biological replicates were conducted for ribosome profiling and mRNA lifetime profiling, respectively. And genes with sufficient expression level (RPKM >1) were subjected to further analysis. The change fold that used in the main text is the average of the two $\log_2$(siYTHDF2/siControl) values. Nonparametric Mann–Whitney U-test (Wilcoxon rank-sum test, two sided, significance level = 0.05) was applied in ribosome profiling data analysis as previous reported[22]. For the analysis of cell viability (Extended Data Fig. 8e), RPF of ribosome profiling data were analysed by Cuffidff version 2.0 for differential expression test, and the genes that differentially expressed ($P < 0.05$) were subjected to Ingenuity Pathway Analysis (IPA, Ingenuity System). RPF was chosen since it may better reflect the translation status of each gene.

Data accession: all the raw data and processed files have been deposited in the Gene Expression Omnibus (http://www.ncbi.nlm.nih.gov/geo). m^{6}A profiling data are accessible under GSE46705 (GSM1135030 and GSM1135031 are input samples whereas GSM1135032 and GSM1135033 are immunoprecipitation samples). All other data are accessible under GSE49339.

RT–PCR. Real-time PCR (RT–PCR) was performed to assess the relative abundance of mRNA. All RNA templates used for RT–PCR were pre-treated with on column DNase I in the purification step. The RT–PCR primers were designed to span exon-exon junctions in order to further eliminate the amplification of genomic DNA and unspliced mRNA. When the examined gene had more than one isoform, only exon–exon junctions shared by all isoforms were selected to evaluate the overall expression of that gene. RT–PCR was performed by using Platinum one-step kit (Invitrogen) with 200–400 ng total RNA template or 10–20 ng mRNA template. *HPRT1* was used as an internal control because: (1) *HPRT1* mRNA did not have m^{6}A peak from m^{6}A profiling data; (2) *HPRT1* mRNA was not bound by YTHDF2 from the PAR-CLIP and RIP sequencing data; (3) *HPRT1* showed relative invariant expression upon YTHDF2 knockdown from the RNA-seq data; (4) *HPRT1* was a house-keeping gene.

YTHDF2: TAGCCAACTGCGACACATTC; CACGACCTTGACGTTCCTTT.

SON: TGACAGATTTGGATAAGGCTCA; GCTCCTCCTGACTTTTTAGCAA.

CREBBP: CTCAGCTGTGACCTCATGGA; AGGTCGTAGTCCTCGCACAC.

PLAC2: AAGCGCTACCACATCAAGGT; CCTCCAACCCAGACTACCTG.

LDLR: GCTACCCCTCGAGACAGATG; CACTGTCCGAAGCCTGTTCT.

HPRT1: TGACACTGGCAAAACAATGCA; GGTCCTTTTCACCAGCAAGCT.

F-luc or F-luc-5BoxB: CACCTTCGTGACTTCCCATT; TGACTGAATCGGAC ACAAGC.

R-luc: GTAACGCTGCCTCCAGCTAC; CCAAGCGGTGAGGTACTTGT.

A combination of knockdown/overexpression/RIP/RT–PCR experiments was conducted to evaluable the occupancy change of YTHDF2 on its RNA targets after MT-A70 (METTL3) knockdown (Extended Data Fig. 5). Two 15-cm plates of HeLa cells were transfected with siControl or siMETTL3 siRNA. After 10 h, the cells were re-seeded. After 14 h, the cells were further transfected with Flag-tagged YTHDF2 plasmid, and collected after another 24 h (in total 48 h knockdown of METTL3, 24 h over-expression of Flag–YTHDF2). Anti-Flag beads were used to separate YTHDF2-bound portion (IP) from unbound portion (flow-through) as described in the RIP section.

Fluorescence microscopy. Fluorescent immunostaining: the protocol of ref. 26 was followed. The cells were grown in an 8-well chamber (Lab-Tek). After treatment indicated in each experiment, the cells were washed once in PBS and then fixed in 4% paraformaldehyde in PBST (PBS with 0.05% Tween-20; prepared by mixing paraformaldehyde with PBST, heat at 60 °C until clear, pH~7.5) at room temperature for 15 min under rotation. The fixing solution was removed, and −20 °C chilled methanol was immediately added to each chamber and incubated for 10 min at room temperature. The cells were rinsed once in PBS and incubated with blocking solution (10% FBS with PBST) for 1 h at room temperature under rotation. After that, the blocking solution was replaced with primary antibody (diluted by fold indicated in Antibodies section in blocking solution) and incubated for 1 h at room temperature (or overnight at 4 °C). After being washed 4 times with PBST (300 µl, 5–10 min for each wash), secondary antibody (1:300 dilution in PBST) was added to the mixture and incubated at room temperature for 1 h. After washing 4 times with PBST (300 µl, 5–10 min for each wash), anti-fade reagent (slowfade, Invitrogen) was added to mount the slides.

FISH in conjugation with fluorescent immunostaining: Stellaris FISH probe with Quasar 570 was used according to the manufacturer's instructions. After the washing step, the sample preparation proceeded to the blocking step of the previous paragraph in the presence of 40 U ml^{-1} of RNase inhibitor. Secondary antibodies were Alexa 488 and Alexa 647 conjugates.

Image capture and analysis: the images were captured by Leica SP5 II STED-CW super-resolution laser scanning confocal microscope, analysed by ImageJ. The colocalization was quantified by JAcoP (ImageJ plug-in) and the Pearson coefficients in main text Fig. 3 were gained under Costes' automatic threshold[40].

Protein co-immunoprecipitation. HeLa cells expressing Flag-tagged YTHDF2, N-YTHDF2, C-YTHDF2 or pcDNA3.0 blank vector were collected by cell lifter (three 15-cm plates for each), and pelleted by centrifuge at 400*g* for 5 min. The cell pellet was resuspended with 2 volumes of lysis buffer (the same as the one used in RIP), and incubated on ice for 10 min. To remove the cell debris, the lysate solution was centrifuged at 15,000 *g* for 15 min at 4 °C, and the resulting supernatant was passed through a 0.22-µm membrane syringe filter. While 50 µl of cell lysate was saved as Input, the rest was incubated with the anti-Flag M2 magnetic beads (Sigma) in ice-cold NT2 buffer (the same as the one used in RIP) for 4 h at 4 °C. Afterwards, the beads was subject to extensive wash with 8 × 1 ml portions of ice-cold NT2 buffer, followed by incubation with the elution solution containing 3 × Flag peptide (0.5 mg ml^{-1} in NT2 buffer, Sigma) at 4 °C for another 2 h. The eluted samples, saved as IP, were analysed by western blotting. For IP samples, each lane was loaded with 2 µg IP portion; and the input lane were loaded with 10 µg Input portion which corresponded to ~1% of overall input.

Tether assay. Basic setting: 100 ng reporter plasmid (pmirGlo or pmirGlo-5BoxB) and 500 ng effecter plasmid (pcDNA-Flag-λ, pcDNA-Flag-Y2Nλ, or pcDNA-Flag-Y2N) were used to transfect the HeLa cells in each well of six-well plate at 60~80% confluency. After 6 h, each well was re-seeded into 96-well plate (1:20) and 12-well plate (1:2). After 24 h, the cells in 96-well plate were assayed by Dual-Glo Luciferase Assay Systems (Promega). Firefly luciferase (F-luc) activity was normalized by *Renilla* luciferase (R-luc) to evaluate the translation of reporter. And samples in 12-well plate were processed to extract total RNA (DNase I digested), followed by RT–PCR quantification. The amount of F-luc mRNA was also normalized by that of R-luc mRNA.

RNA immunoprecipitation: Two 15-cm plates of HeLa cells were transfected with 1 µg pmirGlo-5BoxB reporter and 5 µg pcDNA-Flag-Y2Nλ effecter plasmids for each plate. After 24 h, the samples were processed as described in RIP section. The recovered RNA from Input, IP and FT portions were used in poly(A) tail assay.

RNA decay: 200 ng reporter plasmid (pmirGlo-Ptight-5BoxB) and 1 µg effecter plasmid (pcDNA-Flag-λ, pcDNA-Flag-Y2Nλ, or pcDNA-Flag-Y2N) were used for each 6 cm plate to transfect the HeLa Tet-off cell line (Clontech) in the presence of 400 ng doxycycline (Dox, Clontech). The transcription of F-luc5BoxB was under repression at this stage. After 18 h, the cells in each 6-cm plate were washed twice with PBS, trypsinized, and washed twice with Dox-free media, then split to four equal portions and re-seeded to 12-well plate in Dox-free media. After 4 h pulse transcription of F-luc5BoxB, Dox was added to 400 ng in each well. The first time point ($t = 0$ h) was taken as after 20 min[41], then 2 h, 4 h and 6 h. Total RNA extracted from each sample were used for RT–PCR analysis and Poly(A) tail length assay.

Poly(A) tail length assay. Poly(A) tail length assay was performed by using Poly(A) Tail-Length Assay kit (Affymetrix) as previously reported[7]. The protocol of the manufacture (Extended Data Fig. 7f–l) was followed, with 30 cycles of two-step PCR at the last step, and then visualized on 10% non-denaturing TBE gel. The forward primer of F-luc-5BoxB is 5′-CCGCTGAGCAATAACTAGCA-3′, and the gene-specific reverse primer is 5′-TGCAATTGTTGTTGTTAACTTGTTT-3′. The forward primer of *CREBBP* mRNA is 5′-GTCTTGGGCAATCCAGATGT-3′, and the gene-specific reverse primer is 5′- TTTGAATCCAAGTAGTTTTACCATC -3′.

Antibodies. The antibodies used in this study were listed below in the format of name (application; catalogue; supplier; dilution fold): Rabbit anti-YTHDF1 (Western; ab99080; Abcam; 1,000). Rabbit anti-YTHDF3 (Western; ab103328; Abcam; 1,000). Mouse anti-Flag HRP conjugate (Western; A5892; Sigma; 5000). Rabbit anti-MT-A70 (Western; 15073- 1-AP; Proteintech Group; 3000). Rabbit anti-FTO (Western; 5325-1; Epitomics; 10,000). Goat anti-GAPDH HRP conjugate (Western; A00192; GeneScript; 15,000). Rabbit anti-DCP2 (Western; Ab28658;

Abcam; 1,000). Rabbit anti-m^{6}A (m^{6}A-seq; 202003; Synaptic Systems; 4 μg per seq). Rat anti-Flag (IF; 637304; Biolegend; 300). Mouse anti-DCP1a (IF; WH0055802M6; Sigma; 300). Mouse anti-GW182 (4B6) (IF; ab70522; Abcam; 100). Rabbit anti-DDX6 (IF; a300-461A; Bethyl Lab; 250). Anti-HuR (IF; WH0001994M2; Sigma; 50). Goat anti-eIF3 (N-20) (IF; sc-16377; Santa Cruz Biotech; 100). Mouse anti-CNOT7 (IF; sc-101009; Santa Cruz Biotech; 100). Goat anti-PAN2 (C-20) (IF; sc-82110; Santa Cruz Biotech.; 100). Anti-PARN (IF; ab27778; Abcam; 100). Donkey anti-rat Alexa 488 (IF; A21208; Molecular Probes; 300). Goat anti-rabbit Alexa 647 (IF; A21446; Molecular Probes; 300). Goat anti-mouse Alexa 647 (IF; A21236; Molecular Probes; 300). Donkey anti-goat Alexa 647 (IF; A21447; Molecular Probes; 300).

31. Pillai, R. S., Artus, C. G. & Filipowicz, W. Tethering of human Ago proteins to mRNA mimics the miRNA-mediated repression of protein synthesis. *RNA* **10,** 1518–1525 (2004).
32. Hafner, M. *et al.* PAR-CliP - a method to identify transcriptome-wide the binding sites of RNA binding proteins. *J. Vis. Exp.* **41,** e2034 (2010).
33. Kishore, S. *et al.* A quantitative analysis of CLIP methods for identifying binding sites of RNA-binding proteins. *Nature Methods* **8,** 559–564 (2011).
34. Pearson, W. R., Wood, T., Zhang, Z. & Miller, W. Comparison of DNA sequences with protein sequences. *Genomics* **46,** 24–36 (1997).
35. Trapnell, C., Pachter, L. & Salzberg, S. L. TopHat: discovering splice junctions with RNA-Seq. *Bioinformatics* **25,** 1105–1111 (2009).
36. Anders, S. & Huber, W. Differential expression analysis for sequence count data. *Genome Biol.* **11,** R106 (2010).
37. Trapnell, C. *et al.* Transcript assembly and quantification by RNA-Seq reveals unannotated transcripts and isoform switching during cell differentiation. *Nature Biotechnol.* **28,** 511–515 (2010).
38. Zhang, Y. *et al.* Model-based analysis of ChIP-Seq (MACS). *Genome Biol.* **9,** R137 (2008).
39. Corcoran, D. L. *et al.* PARalyzer: definition of RNA binding sites from PAR-CLIP short-read sequence data. *Genome Biol.* **12,** R79 (2011).
40. Bolte, S. & Cordelieres, F. P. A guided tour into subcellular colocalization analysis in light microscopy. *J. Microsc.* **224,** 213–232 (2006).
41. Clement, S. L. & Lykke-Andersen, J. A tethering approach to study proteins that activate mRNA turnover in human cells. *Methods Mol. Biol.* **419,** 121–133 (2008).

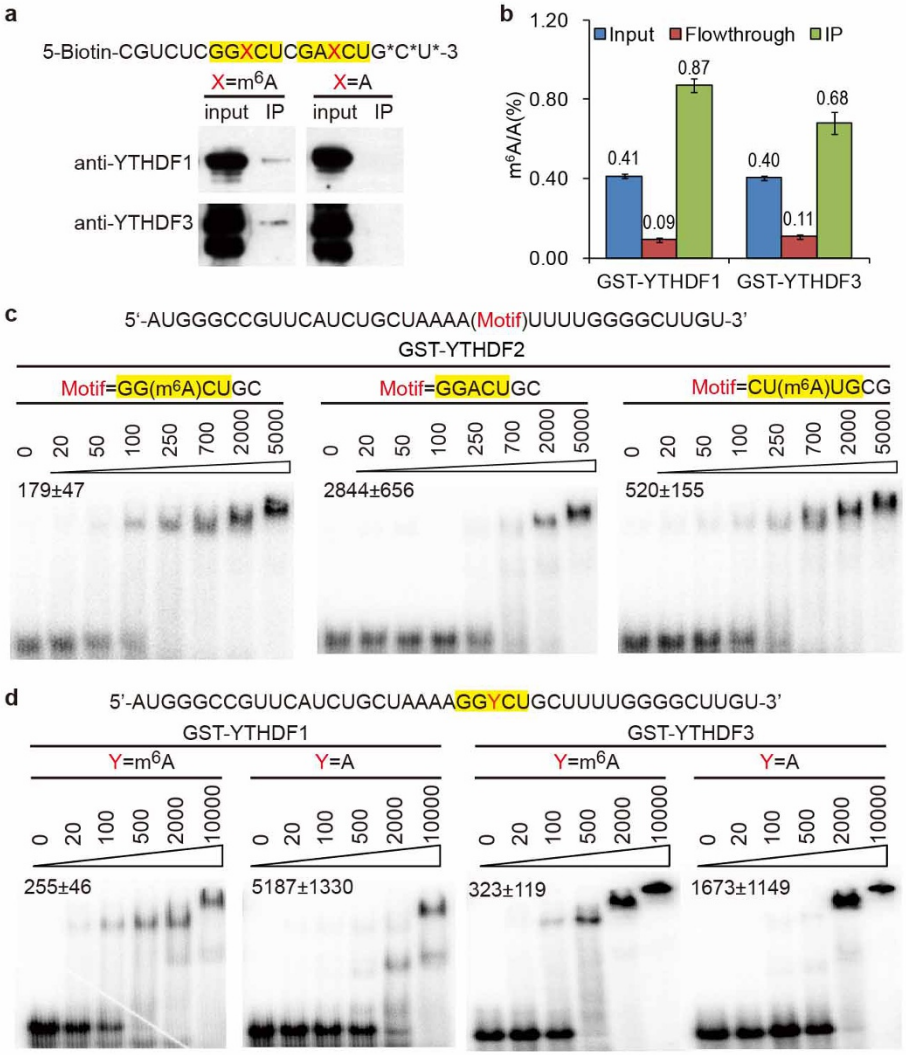

Extended Data Figure 1 | YTH domain family members are m^{6}A-specific RNA binding proteins. **a**, Western blot showing YTHDF1 and YTHDF3 pulled down with an m^{6}A-containing RNA probe. *Thiol-substituted phosphodiester bonds were used to prevent enzymatic cleavage. **b**, LC-MS/MS showing that m^{6}A was enriched in GST–YTHDF1- or GST–YTHDF3-bound mRNA while depleted in the flow-through portion. **c**, **d**, Gel-shift assay measuring the dissociation constant (K_d, nM, indicated at the upper left corner of the gel) of GST-tagged YTH domain family proteins (**c**, YTHDF2; **d**, YTHDF1 and YTHDF3) with methylated and unmethylated RNA probes. 4 nmol RNA probe was labelled with ^{32}P and the protein concentration ranged from 20 nM to 5 μM.

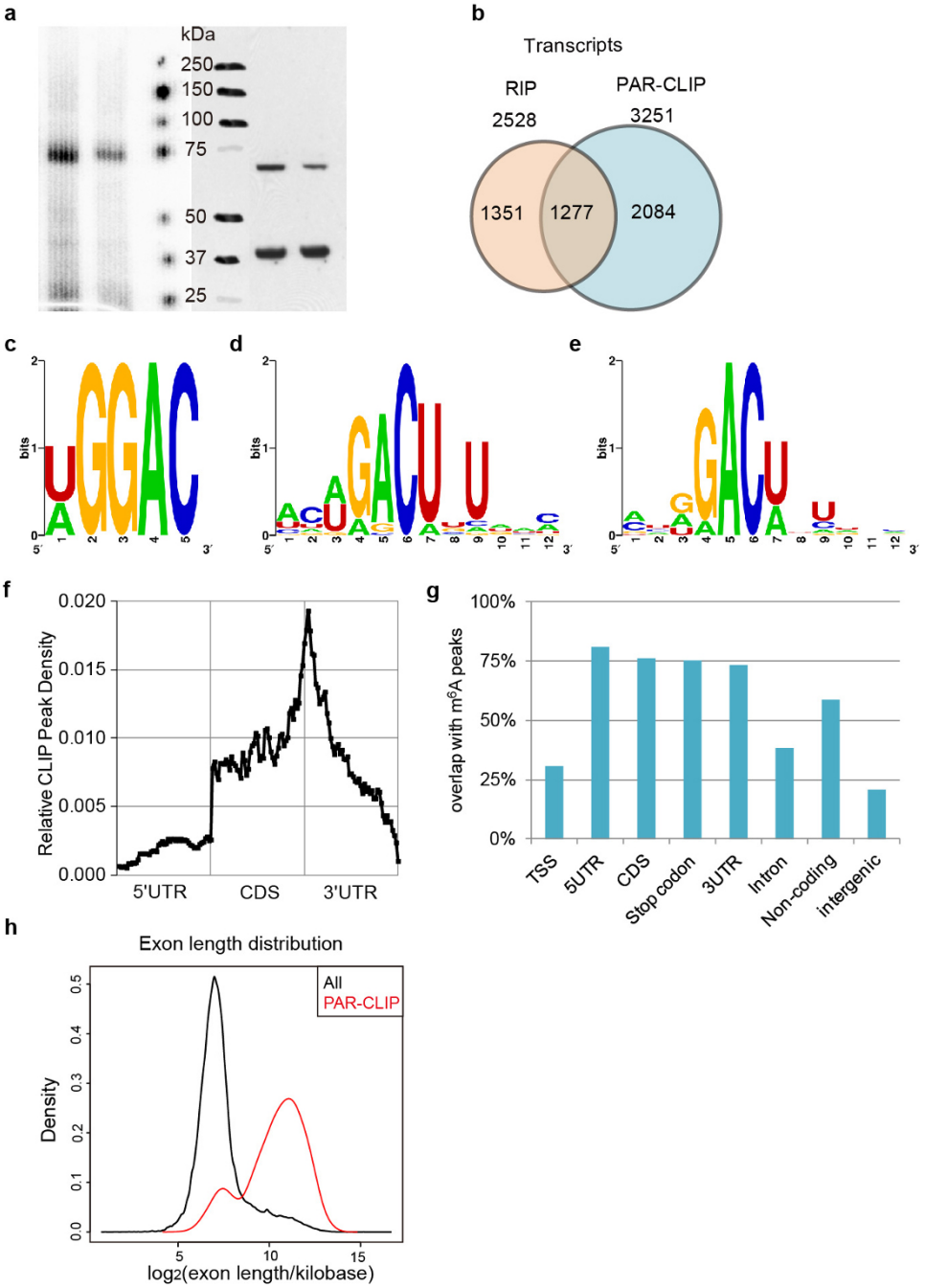

Extended Data Figure 2 | Features and comparisons of YTHDF2 PAR-CLIP data with RIP and m^{6}A-seq. **a**, Left, PAR_CLIP gel image showing ^{32}P-labelled RNA–YTHDF2 complex; right, western blotting of HeLa cell lysate with overexpression of Flag-tagged YTHDF2 (10 μg per lane). Upper band was detected by anti-Flag antibody; lower band was detected by anti-GAPDH antibody. **b**, Overlap of transcripts identified by PAR-CLIP and RIP-seq of YTHDF2. **c**, **d**, YTHDF2 binding motif identified by MEME with top 1,000 scored PAR-CLIP peaks under different motif searching parameters. **c**, With motif length restricted to 5–10 bp, $P = 1.1 \times 10^{-43}$, 183 sites were found under this motif. **d**, The motif length was restricted to 5–12 bp. The motif with lowest P value was shown in main text as Fig. 1c, this motif showed the second lowest P value, $P = 5.1 \times 10^{-14}$, 104 sites were found. **e**, With 7–12 bp, $P = 7.5 \times 10^{-42}$, 231 sites were found under this motif. **f**, Distribution of PAR-CLIP peaks across the length of mRNA. Each region of 5′ UTR, CDS, and 3′ UTR were binned into 50 segments, and the percentage of PAR-CLIP peaks that fall within each bin was determined. **g**, Overlap of YTHDF2 PAR-CLIP peaks with m^{6}A peaks in different sub-transcript regions. Over 70% PAR-CLIP peaks in 5′ UTR, CDS, stop codon, and 3′ UTR regions overlap with m^{6}A peaks (at least 1-bp overlap). In contrast, only 20%~30% of PAR-CLIP peaks in transcription starting sites (TSS) and intergenic regions coincide with m^{6}A peaks. **h**, Enrichment of YTHDF2 PAR-CLIP peaks in long exons. The length distribution of exons that contain YTHDF2 PAR-CLIP peaks (red) shifts to larger size compared with the length distribution of all exons in the human genome (black).

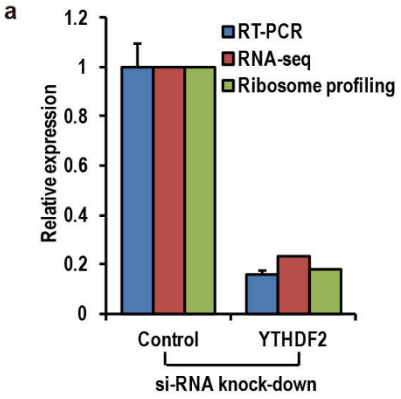

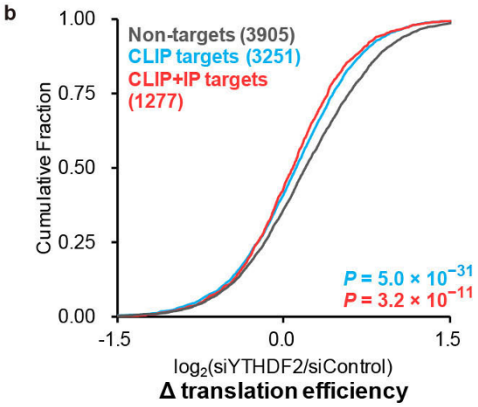

c

Sample	Data set	Frequency	Sum of ranks	Mean of ranks	Median	Groups*
mRNA input	NT	3905	15177599	3886.709	-0.154	A
	CLIP	3251	14242532	4380.907	0.038	B
	CLIP+IP	1277	6141829	4809.577	0.125	C
Ribosome-protected fragments	NT	3905	16129368	4130.440	0.063	A
	CLIP	3251	13633808	4193.727	0.086	A
	CLIP+IP	1277	5798784	4540.943	0.147	B
Translation Efficiency	NT	3905	17393203	4454.085	0.189	B
	CLIP	3251	13147547	4044.155	0.110	A
	CLIP+IP	1277	5021210	3932.036	0.084	A
mRNA lifetime	NT	2400	5333012	2222.088	-0.030	A
	CLIP	2504	8159838	3258.721	0.273	B
	CLIP+IP	966	3738535	3870.119	0.325	C
	NT	2400	4815283	2006.368	-0.030	A
	CLIP=1	1034	2730168	2640.395	0.195	B
	CLIP=2~4	1058	3097145	2927.358	0.286	C
	CLIP≥5	412	1384464	3360.350	0.383	D
	NT	2400	3868749	1611.979	-0.030	A
	5UTR	28	71550	2555.357	0.359	B
	CDS	591	1432600	2424.027	0.319	B
	3UTR	709	1642005	2315.945	0.273	B
	Intron	30	61929	2064.300	0.146	A
	Non-coding	12	31502	2625.167	0.414	B

* group naming follows the sorting of the mean of ranks: A<B<C<D

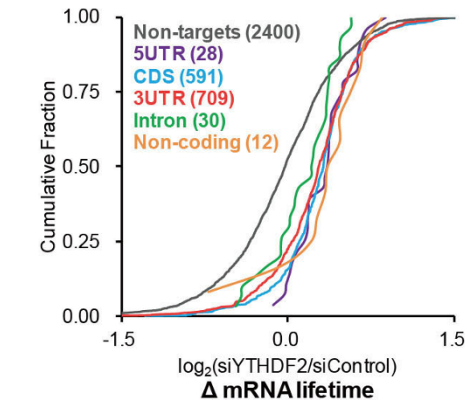

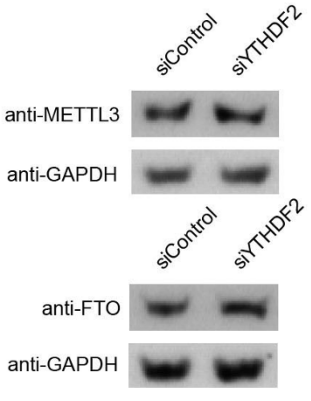

Extended Data Figure 3 | Effects of YTHDF2 knockdown and summary of the sequencing data. **a**, The YTHDF2 knockdown efficiency is about 80% as detected by RT–PCR (error bars, mean ± s.d., $n = 3$, biological replicates) and RNA-seq. Although at current stage we could not identify a reliable antibody for YTHDF2, ribosome-profiling of YTHDF2 did indicate that the translation level of YTHDF2 decreased by 80% after siRNA knockdown. RT–PCR results were normalized to that of GAPDH as an internal control. RNA-seq and ribosome profiling results were calculated by actual RPKM. **b**, YTHDF2 knockdown led to decreased translation efficiency of its targets due to the accumulation of non-translating mRNA. Translation efficiency is calculated as the ratio of ribosome-protected fragments and mRNA input. *P* value was calculated by using Mann–Whitney *U*-test (two-tailed, significance level = 0.05). **c**, Multiple pairwise comparisons (Kruskal–Wallis test) by using the Steel–Dwass–Critchlow–Fligner procedure (two-tailed, significance level = 0.05). **d**, The regional effect of the YTHDF2-binding site is not significant. Cumulative distribution showing mRNA lifetime $\log_2$-fold changes (Δ) between si-YTHDF2 and si-control for non-targets and CLIP-IP common targets with major CLIP peak at 5′ UTR, CDS, 3′ UTR, intron, and non-coding RNA. Except for intron, other regions show similar fold changes (also see Extended Data Fig. 3c). **e**, The m^6A methyltransferase (MT-A70) and demethylase (FTO) remain unchanged with YTHDF2 knockdown.

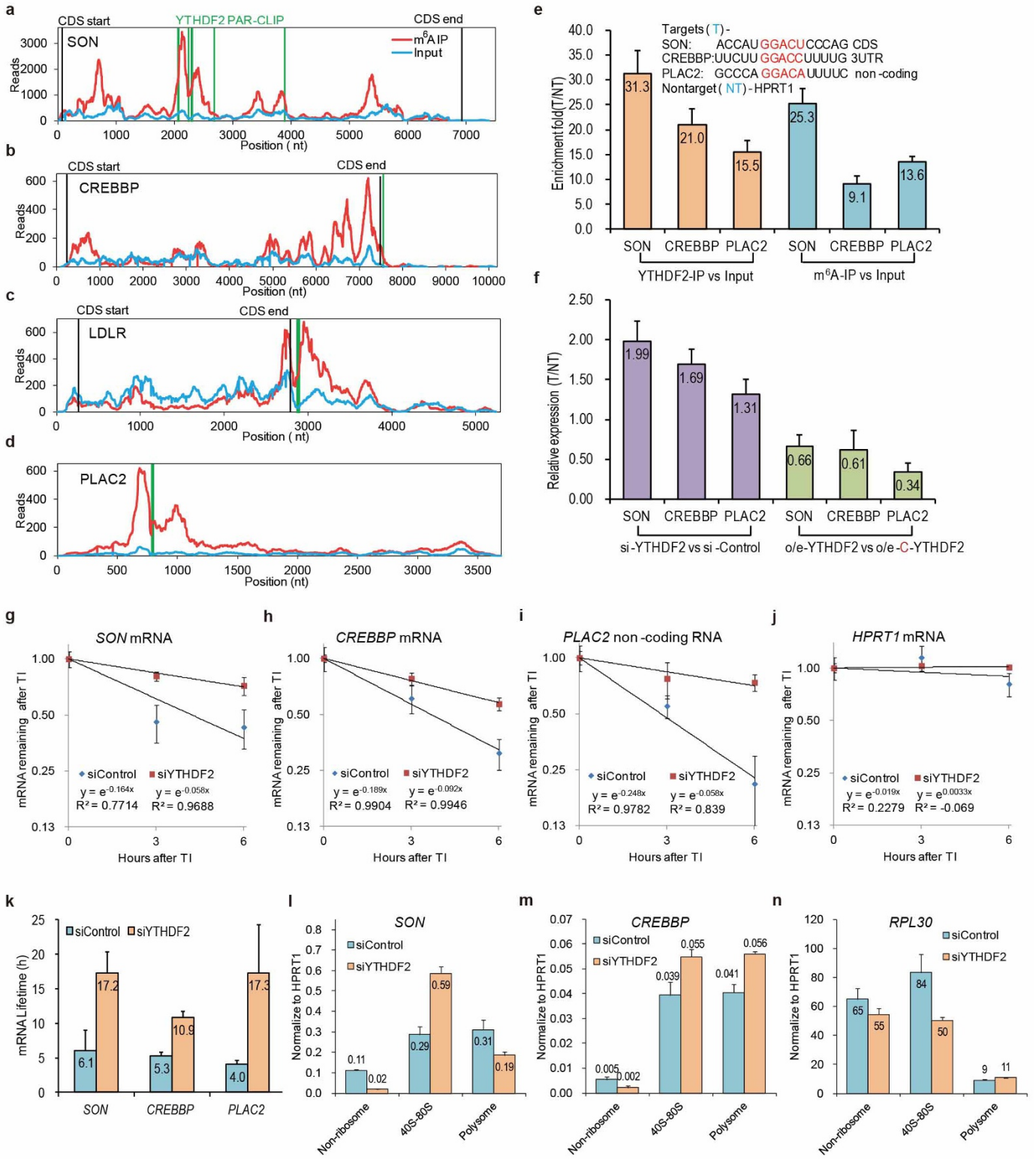

Extended Data Figure 4 | Validation of representative YTHDF2 RNA targets. **a**–**d**, Examples of transcripts harbouring m^{6}A peaks and YTHDF2 PAR-CLIP peaks: *SON* (CDS, **a**), *CREBBP* (3′ UTR, **b**), *LDLR* (3′ UTR, **c**), *PLAC2* (non-coding RNA, **d**). Coverage of m^{6}A immunoprecipitation and input fragments are indicated in red and blue, respectively. YTHDF2 PAR-CLIP peaks are highlighted in green. Black lines signify CDS borders. **e**–**n**, relative RNA level quantified by gene-specific RT–PCR, and error bars shown in these figure panels are mean ± s.d., $n = 6$ (two biological replicates × three technical replicates). **e**, Enrichment fold of *SON*, *CREBBP* mRNA, and *PLAC2* RNA in YTHDF2-RNA coimmunoprecipitation versus RNA–protein input control, and in m^{6}A *in vitro* immunoprecipitation versus mRNA input control. **f**, Relative changes of *SON*, *CREBBP* mRNA, and *PLAC2* RNA in siYTHDF2 sample versus siControl, and overexpression of YTHDF2 versus overexpression of C-YTHDF2. **g**–**k**, Lifetimes of *SON*, *CREBBP* mRNA and *PLAC2* RNA under siYTHDF2 versus siControl. **l**–**n**, YTHDF2 knockdown altered the cytoplasmic distribution of its mRNA targets. The *SON* (**l**) and *CREBBP* (**m**) mRNA levels decreased in the non-ribosome mRNP portion but increased in the 40S–80S portion under siYTHDF2 compared to siControl. However, they showed different changes in the polysome portion. *RPL30* (**n**) is not a target of YTHDF2 and did not show an increase in the 40S–80S portion.

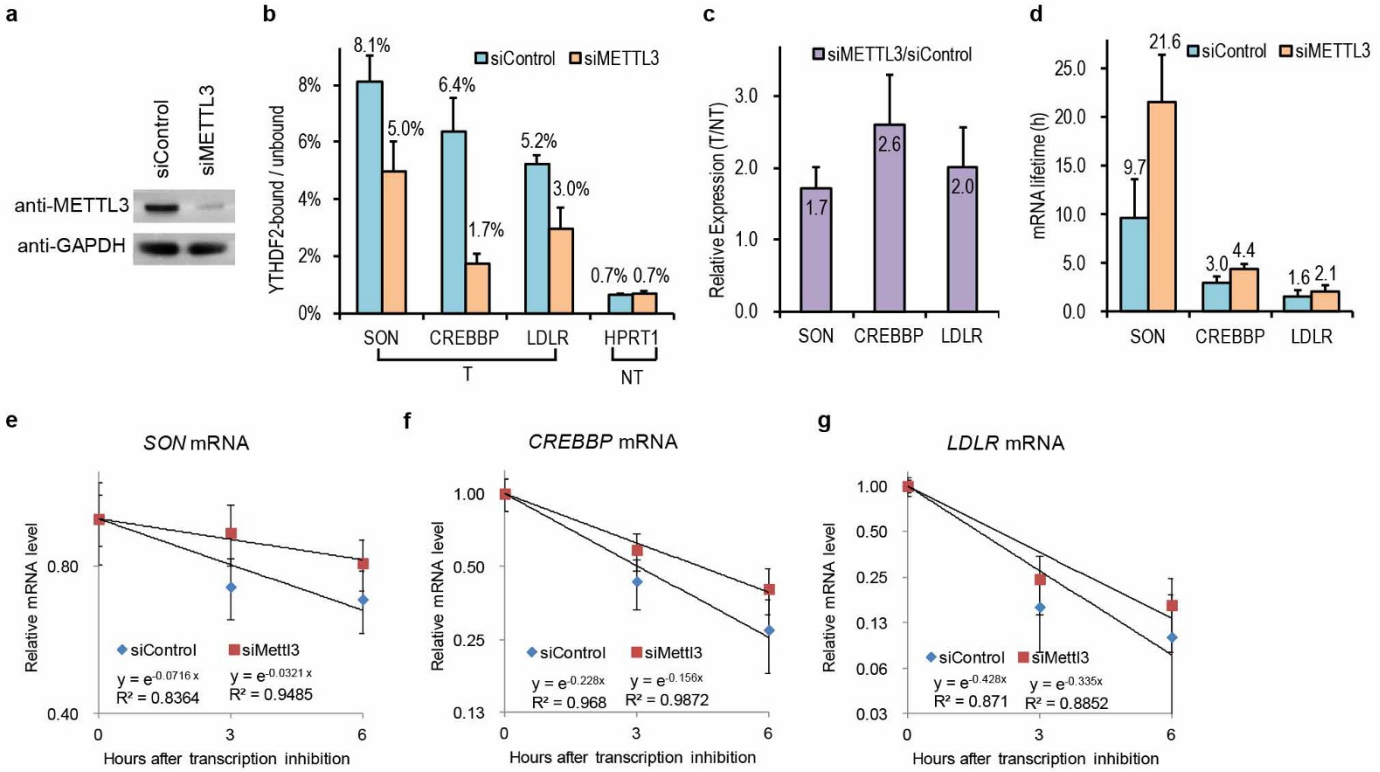

Extended Data Figure 5 | Knockdown of METTL3 (MT-A70) led to decreased binding of YTHDF2 to its targets and increased stability of its target RNAs similar to that of YTHDF2 knockdown. **a**, Western blotting showing that the knockdown efficiency of siMETTL3 at 48 h was ~80%. **b–g**, Relative RNA level quantified by gene-specific RT–PCR, and error bars shown in these figure panels are mean ± s.d., $n = 6$ (two biological replicates × three technical replicates). **b**, Percentages of YTHDF2 targets (*SON*, *CREBBP*, *LDLR*) in YTHDF2-bound portion versus unbound portion decreased significantly after METTL3 knockdown for 48 h. After 24 h transfection of METTL3 siRNA, HeLa cells were transfected with Flag-tagged YTHDF2, and cells were collected after another 24 h. Anti-Flag beads were used to separate YTHDF2-bound portion (IP) from unbound portion (flow-through). Each transcript was quantified by RT–PCR. **c**, Relative changes of *SON*, *CREBBP* and *LDLR* mRNA in siMETTL3 sample versus siControl. **d–g**, Lifetimes of *SON*, *CREBBP*, and *LDLR* mRNA under siMETTL3 versus siControl.

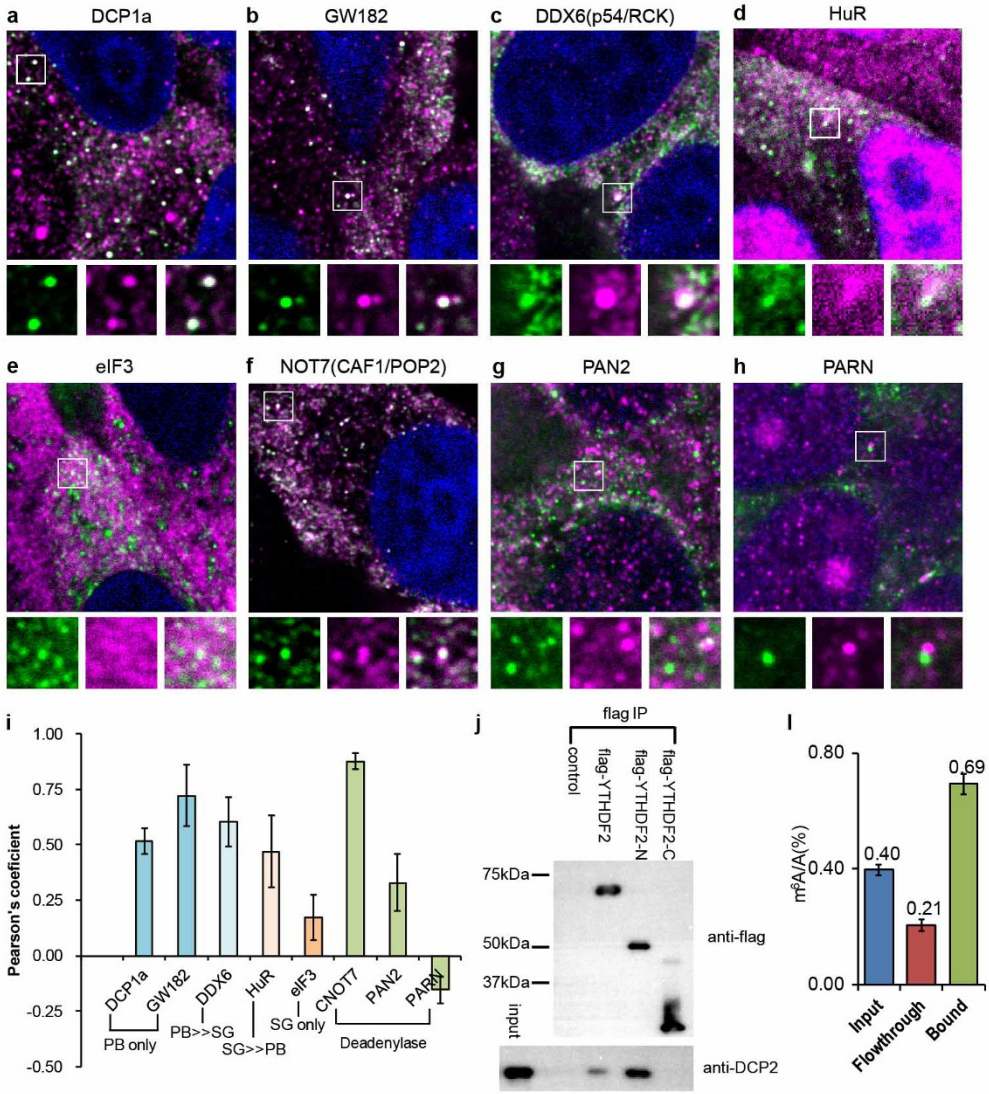

k

Gene	Region (aa)	Length (aa)	YGNQP %	Sequence
TIA-1	290-387	98	66.3	MINPVQQQNQIGYPQPYGQWGQWYGNAQQIGQYMPNGWQVPAYGMY GQAWNQQGFNQTQSSAPWMGPNYGVQPPQGQNGSMLPNQPSGYRVA GYETQ
TIAR	281-375	95	62.1	MTKNFQQVDYSQWGQWSQVYGNPQQYGQYMANGWQVPPYGVYGQP WNQQGFGVDQSPSAAWMGGFGAQPPQGQAPPPVIPPPNQAGYGMASY QTQ
Prion-protein	29-131	103	62.1	GGWNTGGSRYPGQGSPGGNRYPPQGGGGWGQPHGGGWGQPHGGG WGQPHGGGWGQPHGGGWGQGGGTHSQWNKPSKPKTNMKHMAGAAA AGAVVGGLGGYVLG
YTHDF1	284-362	79	57.0	PVPQQAPSPQAAPQPQQVAQPLPAQPPALAQPQYQSPQQPPQTRWVAP RNRNAAFGQSGGAGSDSNSPGNVQPNSAPSV
YTHDF2	288-383	96	56.3	PSQALVQNIGQPTQGSPQPVGQQANNSPPVAQASVGQQTQPLPPPPPQ PAQLSVQQQAAQPTRWVAPRNRGSGFGHNGVDGNGVGQSQAGSGSTP S
YTHDF3	288-388	101	62.4	PPTQPVLPPQTIIQQPQPLIQPPPLVQSQLPQQQPQPPQPQQQQGPQPQ AQPHQVQPQQQQLQNRWVAPRNRGAGFNQNNGAGSENFGLGVVPVSA SPSSV

Extended Data Figure 6 | Co-localization of YTHDF2 with protein markers of P bodies, stress granules, and deadenylation complexes. **a**–**h**, Fluorescence immunostaining of Flag-tagged YTHDF2 (green, anti-Flag, Alexa 488) and other protein markers (DCP1a and GW182 for P bodies and eIF3 for stress granule, DDX6 (also known as RCK/p54) and HuR for both, CNOT7, PAN2, and PARN for deadenylation complex; magenta of Alexa 647 is the colour for the marker, green + magenta = white for the co-localization spot). The scale of the magnified region (while frame) is 1.8 μm × 1.8 μm. **i**, Co-localization between YTHDF2 and different protein markers were characterized by Pearson's coefficient, for each pair, $n = 5\sim7$. YTHDF2 seems to have better co-localization with P bodies than stress granules. It also seems to co-localize best with CNOT7 (also known as CAF1 or POP2) which is a subunit of the CCR4-NOT deadenylation complex. **j**, Western blotting results showing that immunoprecipitation (IP) of Flag-tagged full length YTHDF2 and N-YTHDF2 (N-terminal domain) also pulled down the P-body marker DCP2, but not with mock control or C-YTHDF2 (the C-terminal domain). For IP samples, each lane was loaded with 2 μg IP portion; and the input lane was loaded with 10 μg input portion which corresponded to ~1% of overall input). **k**, Comparison of P/Q/N (highlighted) rich regions of YTHDF1-3 with other aggregation-prone proteins. **l**, C-YTHDF2 is capable of selective binding of m^6A-containing RNA. LC-MS/MS showing that m^6A-containing RNA was enriched in the His6-tagged C-YTHDF2-bound mRNA while reduced in the flow-through portion. Error bars shown in the figure are mean ± s.d., $n = 4$ (two biological replicates × two technical replicates).

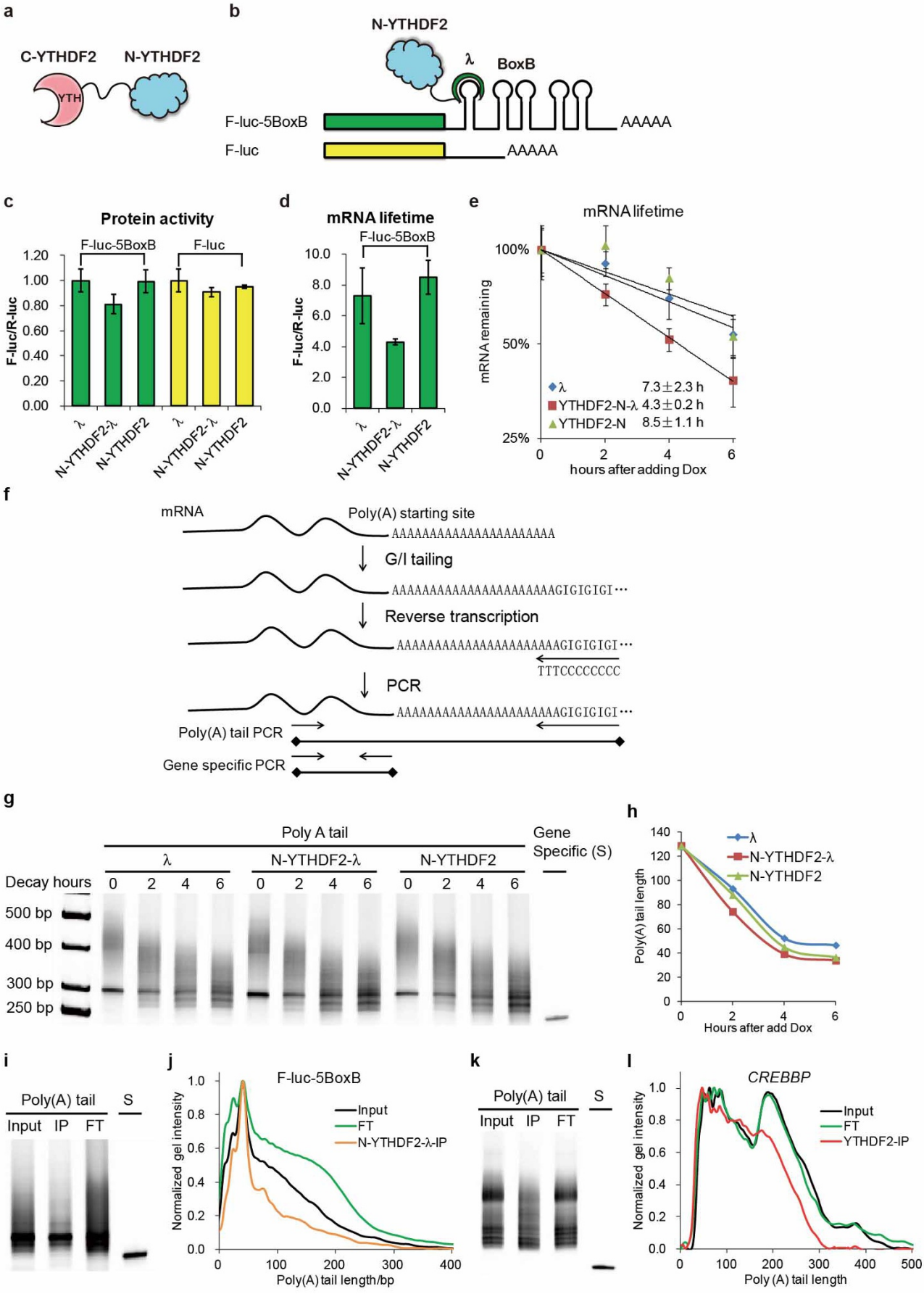

Extended Data Figure 7 | Tether assay of the N-terminal domain of YTHDF2. **a**, Structural presentation of the two domains of YTHDF2. **b**, Scheme of the reporter assay: the RNA reporter vector encodes firefly luciferase (F-luc) as the primary reporter and *Renilla* luciferase (R-luc) on the same plasmids acting as transfection control for normalization. Five Box B RNA elements were inserted at the 3′ UTR of F-luc as positive tether reporter (noted as F-luc-5BoxB); the effecter was a fusion of N-YTHDF2 and λ peptide which recognizes Box B with high affinity. **c**, The F-luc luciferase activity (protein translation) for N-YTHDF2–λ was reduced by ~20% compared to that of N-YTHDF2 and λ controls. Error bars shown in the panel are mean values ± s.d. from $n = 8$ (biological replicates). **d**, **e**, The reporter mRNA lifetime was significantly reduced (~40%) when bound by N-YTHDF2–λ as compared to the controls of N-YTHDF2 and λ. Doxycycline (Dox, 400 ng μl^{-1}) was used to inhibit transcription of the reporter. 18 h post transfection of reporter and effecters, Dox was removed to allow a pulse transcription of F-luc-5BoxB for 4 h. Then Dox was added back and the samples were collected at indicated time point. The amounts of F-luc-5BoxB were determined by RT–PCR, normalized to R-luc, then for each time series, samples at $t = 0$ h were set as 100%. Error bars shown in the panel are mean ± s.d., $n = 6$ (two biological replicates × three technical replicates). **f**, Scheme of poly(A) tail length assay. **g**, **h**, Tethering N-YTHDF2 to the reporter mRNA does not significant trigger deadenylation of the reporter. The PCR products of reporter poly(A) tail were visualized in 10% TBE gel stain (**g**) and no significant difference of the deadenylation rate was observed (**h**). **i**–**l**, Shorter poly(A) tail lengths were observed in the YTHDF2-bound fraction for the N-YHTDF2-tethered reporter RNA (**i** and **j**) as well as the native target RNA *CREBBP* (**k** and **l**). Tether reporter F-luc-5BoxB and Flag-tagged YTHDF2-N-λ (**i**) or full length Flag-tagged YTHDF2 (**k**) were expressed in HeLa cells, and subjected to immunoprecipitation with anti-Flag beads. RNA recovered from input, IP and flow-through were further processed and the final PCR products for F-luc-5BoxB (**i**) or *CREBBP* (**k**) were visualized in 10% TBE gel. **j** and **l**, each lane were re-plotted against base pair, after *log* fitting of relative gel mobility with base pairs.

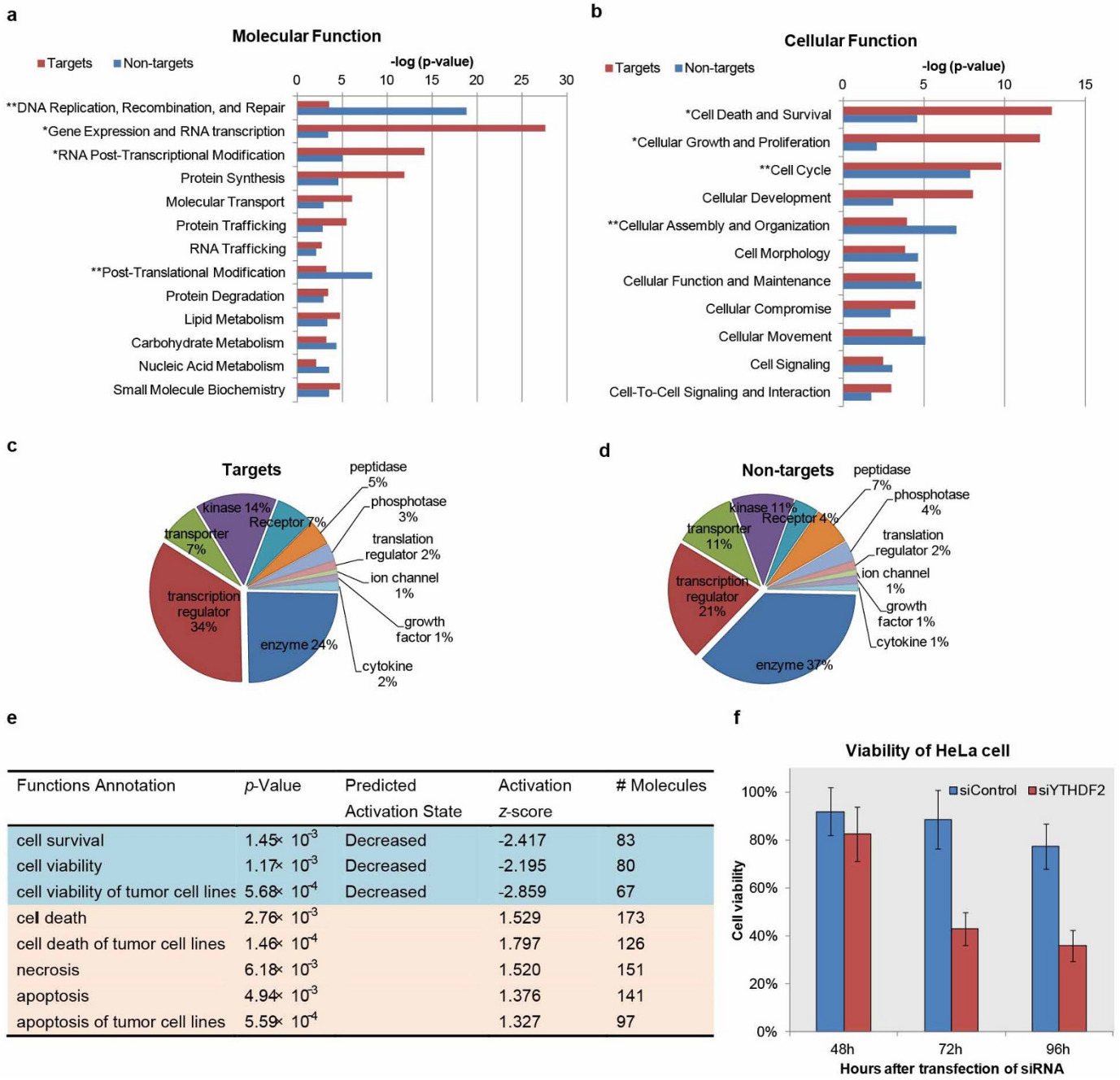

Functions Annotation	*p*-Value	Predicted Activation State	Activation *z*-score	# Molecules
cell survival	1.45×10^{-3}	Decreased	-2.417	83
cell viability	1.17×10^{-3}	Decreased	-2.195	80
cell viability of tumor cell lines	5.68×10^{-4}	Decreased	-2.859	67
cell death	2.76×10^{-3}		1.529	173
cell death of tumor cell lines	1.46×10^{-4}		1.797	126
necrosis	6.18×10^{-3}		1.520	151
apoptosis	4.94×10^{-3}		1.376	141
apoptosis of tumor cell lines	5.59×10^{-4}		1.327	97

Extended Data Figure 8 | Cellular function of YTHDF2. **a**, **b**, The top molecular function of YTHDF2 targets is "Gene Expression and RNA Transcription", and the top cellular function is "Cell Death and Survival". Ingenuity Pathway Analysis of function category of YTHDF2 targets and non-targets revealed that the two gene groups are heterogeneous in their functional composition. (*top two functions for YTHDF2 targets and **top two functions for YTHDF2 non-targets.). **c**, **d**, Pie charts of molecular types of differentially expressed YTHDF2 targets (**c**) versus non-targets (**d**) upon YTHDF2 knockdown. Differentially expressed genes (P value <0.05) caused by YTHDF2 knockdown were grouped to YTHDF2 targets (796 gene) and non-targets (1554) based on their presence or absence in YTHDF2 PAR-CLIP binding sites, and subject to Ingenuity Pathway Analysis (the category "other" was not shown). The results show that the group of YTHDF2 targets is transcription regulators whereas that of non-targets is enzyme, indicating that m^6A may significantly affect gene expression via tuning mRNA stabilities of transcription factors through YTHDF2. **e**, **f**, YTHDF2 knockdown led to reduced cell viability. The IPA analysis of ribosome profiling data of YTHDF2 knockdown (48 h) versus control predicts decreased cell viability (**e**). Ribosome profiling data was chosen since it may better reflect the translation status. MTT assay provided experimental evidence of reduced cell viability upon YTHDF2 knockdown. P values that were calculated from Student's t-test were 0.036, 4.7×10^{-4}, and 9.4×10^{-4}, at 48 h, 72 h and 96 h respectively (**f**). Error bars shown in the figure are mean ± s.d., $n = 10$ (biological replicates).

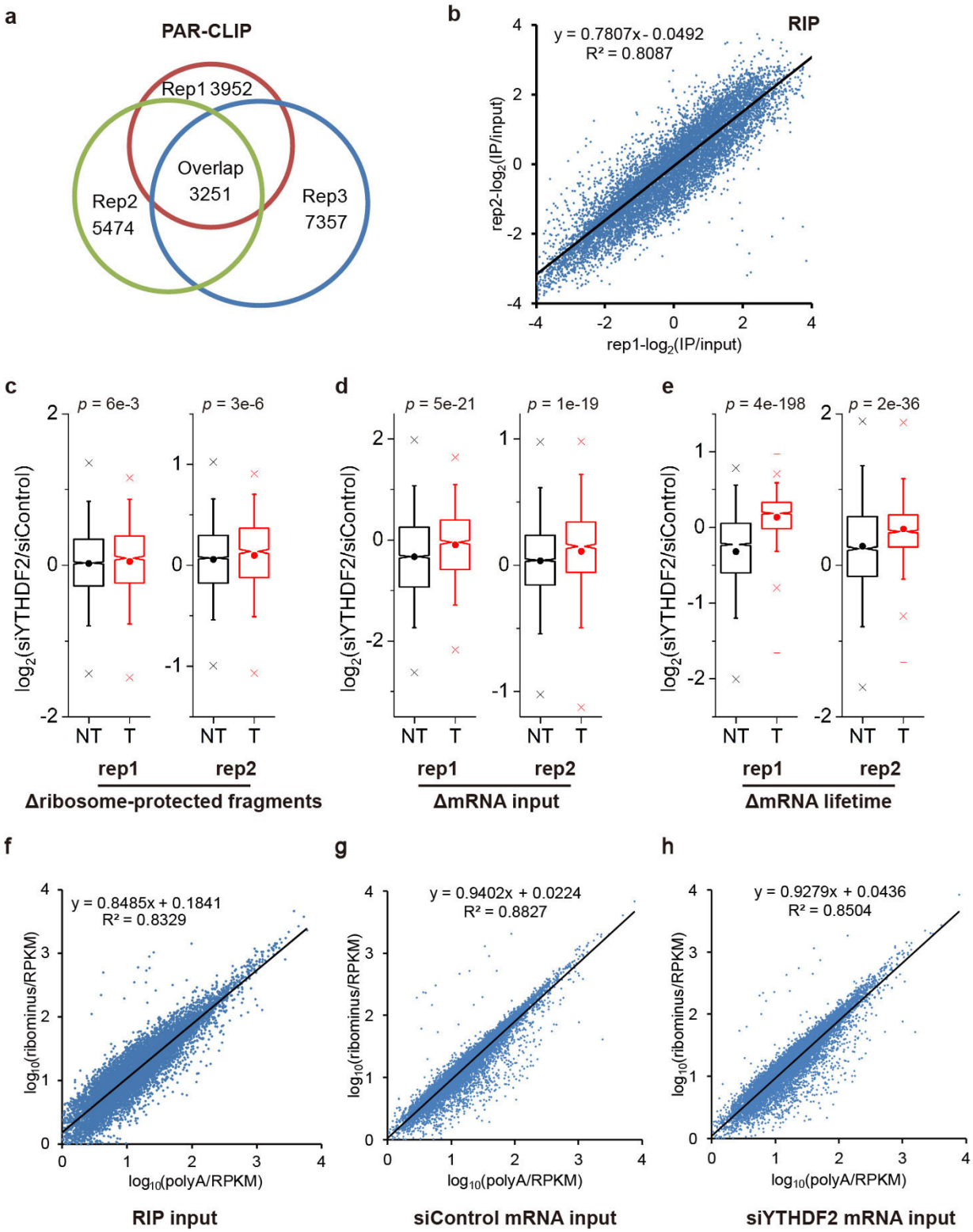

Extended Data Figure 9 | Comparisons of sequencing data with replicates. **a**, Overlap of three biological replicates (rep1–rep3) for PAR-CLIP. Numbers showing the sum of genes identified in each sample. **b**, Correlation of enrichment fold as $\log_2$(IP/input) between two technical RIP replicates. In rep1 the input mRNA was purified by poly(dT) beads, whereas in rep2 the input RNA was processed by rRNA removal. **c**–**e**, Box plot showing consistent results from two biological replicates that were conducted for ribosome profiling and mRNA lifetime profiling, respectively. For mRNA lifetime profiling, rep1 was normalized by spike-in control that was proportional to cell numbers, whereas rep2 was normalized by spike-in that was proportional to total RNA concentrations. Despite the technical variations, YTHDF2 knockdown resulted in significant lifetime increase of its targets. (T, 1,277 CLIP+RIP targets; NT, 3,905 non-targets; box, the first and third quartiles; notch, the median; dot in the box: the data average; whisker, 1.5 × standard deviation; cross, the 1 and 99 percentiles; short line, the maximum and minimum; *P* values were calculated by Mann–Whitney *U*-test, two-tailed, significant level = 0.05). **f**–**h**, Correlation of RPKM between technical mRNA input samples prepared by poly(A) selection (*x* axis) and by rRNA removal (*y* axis), which are comparable to the variations between biological replicates that prepared by the same mRNA selection method.

Extended Data Table 1 | Summary of the sequencing samples

Experiment	Sample / replicates	Mapped Reads
PAR-CLIP	rep1	22398274
	rep2	16469620
	rep3	18340002
m^6A profiling	rep1-input	33037301
	rep1-IP	48299395
	rep2-input	28182497
	rep2-IP	46985896
RIP	IP-rep1	13956595
	IP-rep2	6658433
	input polyA	13995632
	input ribominus	11201129
Ribosome profiling	rep1-SiControl-RPF	6153002
	rep1-SiControl-input-polyA	24693835
	rep1-SiYTHDF2-RPF	4396160
	rep1-SiYTHDF2-input-polyA	23772645
	rep2-SiControl-RPF	10302755
	rep2-SiControl-input-polyA	11276363
	rep2-SiControl-input-ribominus	7336313
	rep2-SiYTHDF2-RPF	9830313
	rep2-SiYTHDF2-input-polyA	9525286
	rep2-SiYTHDF2-input-ribominus	14030008
mRNA lifetime profiling	rep1-SiControl-TI-0h	19703956
	rep1-SiControl-TI-3h	17066177
	rep1-SiControl-TI-6h	25105141
	rep1-SiYTHDF2-TI-0h	23291878
	rep1-SiYTHDF2-TI-3h	18905279
	rep1-SiYTHDF2-TI-6h	27471654
	rep2-SiControl-TI-0h	9709614
	rep2-SiControl-TI-3h	10252359
	rep2-SiControl-TI-6h	13315823
	rep2-SiYTHDF2-TI-0h	9996766
	rep2-SiYTHDF2-TI-3h	11123149
	rep2-SiYTHDF2-TI-6h	7543209